EIT KIC InnoEnergy Master's Programme

Renewable Energy - RENE

MSc Thesis

Identifying opportunities for developing CSP and PV-CSP hybrid projects under current tender conditions and market perspectives in MENA – benchmarking with PV-CCGT

Author: Osama Ali Zaalouk

Supervisors:

Principal supervisor: Prof. Ivette Rodriguez / Universitat Politècnica de Catalunya (UPC)

Industrial supervisor: Rafael Guédez, PhD / Kungliga Tekniska Högskolan (KTH)

Session: September 2016

Escola Tècnica Superior d'Enginyeria Industrial de Barcelona
UNIVERSITAT POLITÈCNICA DE CATALUNYA

MSc RENE is a cooperation between

Universitat Politècnica de Catalunya, Spain | KTH-Royal Institute of Technology, Sweden
Instituto Superior Técnico, Portugal | École Polytechnique (ParisTech), France

Abstract

Concentrating solar power (CSP) is one of the promising renewable energy technologies provided the fact that it is equipped with a cost-efficient storage system, thermal energy storage (TES). This solves the issue of intermittency of other renewable energy technologies and gives the advantage of achieving higher capacity factors and lower levelized costs of electricity (LCOE). This is the main reason why solar tower power plants (STPP) with molten salts and integrated TES are considered one of the most promising CSP technologies in the short term [1]. On the other hand, solar photovoltaic (PV) is a technology whose costs have been decreasing and are expected to continue doing so thus providing competitive LCOE values, but with relatively low capacity factors as electrical storage systems remain not cost-effective. Combining advantages and eliminating drawbacks of both technologies (CSP and PV), Hybridized PV-CSP power plants can be deemed as a competitive economic solution to offer firm output power when CSP is operated smartly so that its load is regulated in response to the PV output. Indeed previous works, have identified that it would allow achieving lower LCOEs than stand-alone CSP plants by means of allowing it to better utilize the solar field for storing energy during the daytime while PV is used [1].

On the fossil-based generation side, the gas turbine combined cycle (CCGT) occupies an outstanding position among power generation technologies. This is due to the fact that it is considered the most efficient fossil fuel-to-electricity converter, in addition to the maturity of such technology, high flexibility, and the generally low LCOE, which is largely dominated by fuel cost and varies depending on the natural gas price at a specific location. Obviously, the main drawback is the generated carbon emissions. In countries rich in natural gas resources and with vast potential for renewable energies implementation, such as the United Arab Emirates (UAE), abandoning a low LCOE technology with competitively low emissions – compared to coal or oil - and heading to costly pure renewable generation, seems like an aggressive plan. Therefore, hybridizing CCGT with renewable generation can be considered an attractive option for reducing emissions at reasonable costs. This is the case of the UAE with vast resources of both natural gas and solar energy.

Previous work have shown the advantages of hybrid PV-CCGT and hybrid PV-CSP plants separately [1][2]. In this thesis, CSP and the two hybrid systems are compared on the basis of LCOE and CO2 emissions for a same firm-power capacity factor when considering a location in the UAE. The results are compared against each other to highlight the benefits of each technology from both environmental and economic standpoints and provide recommendations for future work in the field.

The techno-economic analysis of CSP (STPP with TES), PV-CSP(STPP with TES) and PV-CCGT power plants have been performed by DYESOPT, an in-house tool developed in

KTH, which runs techno-economic performance evaluation of power plants through multi-objective optimization for specific locations[1]. For this thesis, a convenient location in the UAE was chosen for simulating the performance of the plants. The UAE is endowed by the seventh-largest proven natural gas reserves and average to high global horizontal irradiation (GHI) and direct normal irradiation (DNI) values all year round, values considered to be lower than other countries in the MENA region due to its high aerosol concentrations and sand storms. The plants were designed to provide firm power in two cases, first as baseload, and second as intermediate load of 15 hours from 6:00 until 21:00. The hours of production were selected based on a typical average daily load profile.

CSP and PV-CSP model previously developed by [3][1] were used. Ideally in the PV-CSP model, during daytime hours the PV generation is used for electricity production, covering the desired load, while CSP is used partly for electricity production and the rest for storing energy in the TES. Energy in the TES system is then used to supply firm power during both periods of low Irradiance and night hours or according to need.

A PV-CCGT model has been developed which operates simultaneously, prioritizing the availability of PV while the CCGT fulfils the remaining requirement. There is a minimum loading for the CCGT plant which is determined by the minimum possible partial loading of the gas turbine restricted by the emission constraints. Accordingly, in some cases during operation PV is chosen to be curtailed due to this limitation.

The main results of the techno-economic analysis are concluded in the comparative analysis of the 3 proposed power plant configurations, where the PV-CCGT plant is the most economic with minimum LCOE of 86 USD/MWh, yet, the least preferable option in terms of carbon emissions. CSP and PV-CSP provided higher LCOE, while the PV-CSP plant configuration met the same capacity factor with 11% reduction in LCOE, compared to CSP.

Acknowledgements

Firstly, I would like to express my deepest appreciation to my supervisor Rafael Guédez for the support he provided during the course of this master thesis. Secondly, I would like to thank Dr. Björn Laumert and the Solar Research Group at KTH for the great opportunity of joining the group during this work. It has been a great pleasure and an experience enriched with knowledge, excitement and fun. I would like to thank equally Prof. Ivette Rodruigez from UPC for accepting the supervision of my MSc. thesis and for her usual support.

Special thanks to KIC InnoEnergy for providing me this opportunity of a 2 year Masters' program in two of Europe's most beautiful cities: Stockholm and Barcelona. Thanks to all my friends whom I met along those 2 years that were a true inspiration and like family when abroad.

Finally, I must express my very profound gratitude to my family back home, my parents, wife, parents in law, siblings and children for providing me with unfailing support and continuous motivation throughout my years of study. This accomplishment would not have been possible without them. Thank you.

Nomenclature

a-Si	Amorphous Silicon
AC	Alternating Current
ACC	Air-Cooled Condenser
BOT	Build Operate and Transfer
C	Compressor
c-Si	Crystalline silicon
CapEx	Capital Expenditure
CC	Combined Cycle
CCGT	Combined Cycle Gas Turbine
CCS	Carbon Capture and Sequestration
CdTe	Cadmium Telluride
CF	Capacity Factor
CIGS	Copper Indium Gallium Selenide
CO	Carbon Monoxide
CO_2	Carbon Dioxide
COP21	21st Conference Of Parties
CPF	Carbon Price Floor
CR	Central Receiver
CSP	Concentrating Solar Power
CT	Cold Tank
DA	Deaerator
DC	Direct Current
DEWA	Dubai Electricity and Water Authority
DNI	Direct Normal Irradiation
DSCE	Dubai Supreme Council of Energy
DYESOPT	Dynamic Energy System Optimizer
EC	Economizer
EIA	Energy Information Administration
ENG	Emirates National Grid
EPC	Engineering, Procurement and Construction
ESIA	Emirates Solar Industry Association
EV	Evaporator
GCC	Gulf Cooperation Council

GHG	Green House Gases
GHI	Global Horizontal Irradiation
GT	Gas Turbine
HPT	High Pressure Turbine
HT	Hot Tank
HTF	Heat Transfer Fluid
HRSG	Heat Recovery Steam Generator
IPP	Independent Power Producer
IWPP	Independent Water and Power Producer
KPI	Key Performance Indicator
KTH	Kungliga Tekniska Högskolan
LCOE	Levelized Cost of Electricity
LFR	Linear Fresnel Reflector
LPT	Low Pressure Turbine
Matlab	Matrix Laboratory
MENA	Middle East and North Africa
MOO	Multi Objective Optimization
NG	Natural Gas
NOx	Mono-Nitrogen oxides
NREL	National Renewable Energy Laboratory
O&M	Operation and Maintenance
OEM	Original Equipment Manufacturer
OpEx	Operational Expenditure
PB	Power Block
PID	Proportional, Integral and Derivative
PPA	Power Purchase Agreements
PT	Parabolic Trough
Pwc	PricewaterhouseCoopers
PWPA	Power and Water Purchase Agreements
PV	Phtovoltaics
R	Receiver
RE	Renewable Energy
RH	Reheater
SF	Solar Field

SH	Superheater
SM	Solar Multiple
SPV	Special Purpose Vehicle
SS	Solar Share
STTP	Solar Tower Power Plant
T	Turbine
TES	Thermal Energy Storage
TMY	Typical Meteorological Year
UAE	United Arab Emirates

Table of Contents

List of Figures

List of Tables

1. Introduction

The total electricity demand of the globe is rising every year, which is directly reflected in the generation capacities installed. According to EIA report, world electricity generation is projected to reach 36.5 trillion kWh by the year 2040, from 21.6 trillion kWh in 2012, representing an increase of 69%[4]. The energy mix of 2012 as shown in figure 1, dominated by fossil fuels, representing 67% of the total generation followed by renewable energy (including hydro) with 29% and nuclear with 12%. The evolution of this energy mix is in the favor of increasing renewable energy (RE) penetration in the mix, on comparing the energy mix of 2012 to that in 2040, the increase in RE penetration is obvious to be of about 32%[4]. According to the COP21 the scenario targeted is well below 2ºC which accounts for huge investments in power generation sector in RE [5].

There are many reasons for developing these technologies and increasing the clean energy percentage in the energy mix of the country. It depends on the location resources, energy dependency, climate change, opportunity cost, pollution, depletion of fossil fuel resources, and many other reasons.

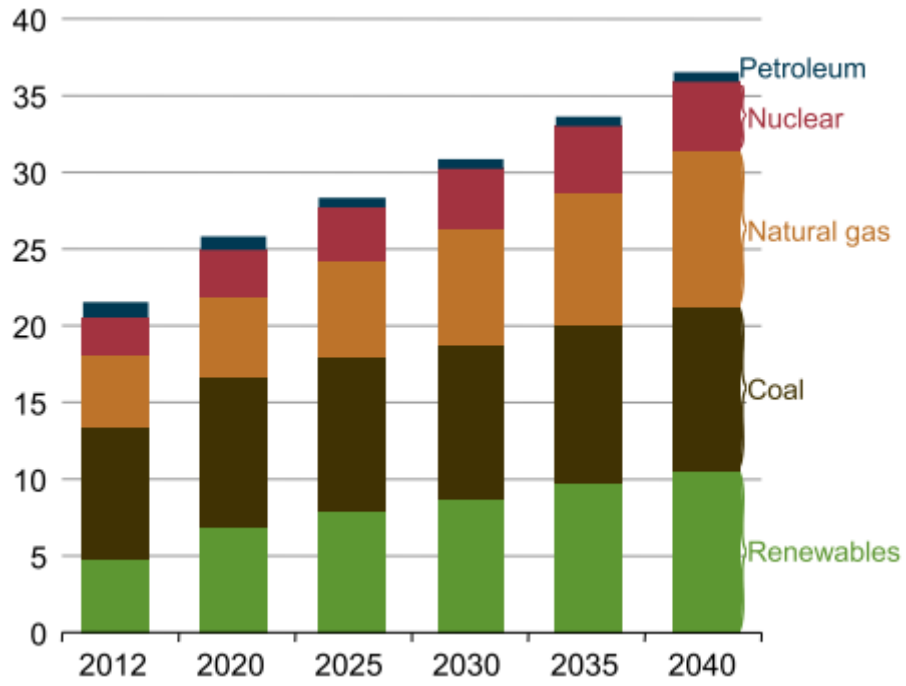

Figure 1. World net electricity generation by fuel [4]

At the early development stage of renewable energy technologies entering the energy mix and the development of these technologies, governments had to subsidize and create policies in favor of the development of such technologies. Nowadays there are some technologies that are already feasible without any subsidies from the government and provide better feasibility than fossil fuel fired technologies.

In this study, the renewable resource of concern is Solar Energy. Solar Energy is the most abundant resource on earth, which is harnessed directly through solar radiation, and indirectly through other forms as wind, hydro (rain), and biomass [6]. As well as fossil fuels as of oil, natural gas, coal, and wood are all formed by photosynthesis, which is a result of solar energy. The Earth atmosphere intercepts 1.75×10^5 TW, out of which 1.05×10^5 TW reaches the earth's surface, considering 60% transmittance. The irradiance on 1% of the earth's surface could provide a resource base of 105 TW through a conversion efficiency of only 10% [7]. For the time being, the technologies that allow harnessing solar energy are basically 2 technologies: Solar photovoltaics (PV) and Solar thermal power, including low and high temperature applications, such as domestic solar water heaters and concentrating solar power (CSP) generation, respectively.

Concentrating solar power (CSP) is one of the promising renewable energy technologies provided the fact that it is equipped with a cost-efficient storage system, thermal energy storage (TES). This solves the issue of intermittency of other renewable energy technologies and gives the advantage of achieving higher capacity factors and lower levelized costs of electricity (LCOE). This is the main reason why solar tower power plants (STPP) with molten salts and integrated TES are considered one of the most promising CSP technologies in the short term[8]. On the other hand, solar photovoltaic (PV) is a technology whose costs have been decreasing and are expected to continue doing so thus providing competitive LCOE values, but with relatively low capacity factors as electrical storage systems remain not cost-effective. Combining advantages and eliminating drawbacks of both technologies (CSP and PV), Hybridized CSP-PV power plants can be deemed as a competitive economic solution to offer firm output power when CSP is operated smartly so that its load is regulated in response to the PV output. Indeed previous works by the authors have identified that it would allow achieving lower LCOEs than stand-alone CSP plants by means of allowing it to better utilize the solar field for storing energy during the daytime while PV is used. [9]

On the fossil-based generation side, the gas turbine combined cycle (CCGT) occupies an outstanding position among power generation technologies. This is due to the fact that it is considered the most efficient fossil fuel-to-electricity converter reaching 60% for the advanced cycles, in addition to the maturity of such technology, high flexibility, the generally low LCOE, which is largely dominated by fuel cost and varies depending on the natural gas price at a specific location. Obviously, the main drawback is the generated carbon emissions. [10]

In this study, power generation cycles involving the previously mentioned technologies CSP, PV and CCGT will be analyzed thoroughly in terms of theory of operation,

modelling, plant design, dynamic performance and feasibility study. A comparative analysis will be performed afterwards, highlighting the pros and cons of each technology from a technical and economic perspective.

The Middle East is a very interesting region to be considered, when it comes to renewable energy and fossil fuel resources. According to the World Energy Resources report 2013 issued by the World Energy Council, This region is endowed with 41% of the world's natural gas proved reserves and 48.1% of the world oil proved reserves [11]. In terms of renewable resources, the most significant resource is solar energy as the Middle East and North Africa lies in the Sun-belt region [12]. The United Arab Emirates will be considered the case study for this work where the previously mentioned technologies are heavily used (CCGT), or of high potential as (PV and CSP). This study considers actual market perspectives and current tender conditions.

1.1. Previous work

There have been many previous research work about simulation and optimization of PV-CSP power plants, which comes to one part of this thesis; While the uniqueness of this work is in the benchmarking of optimized CSP, PV-CSP plant with optimized hybrid PV-CCGT plant, for the UAE.

- **THERMO-ECONOMIC EVALUATION OF SOLAR THERMAL AND PHOTOVOLTAIC HYBRIDIZATION OPTIONS FOR COMBINED-CYCLE POWER PLANTS**, by James Spelling and Björn Laumert, 2015
  This paper compares 3 different configurations of hybridized combined cycles with gas turbine (CCGT), which are: Solar PV with combined cycle (SPVCC), Integrated solar with combined cycle (ISCC), where the heat energy from the solar field is input to the steam cycle, and finally the Hybrid gas turbine combined cycle (HGTCC), where the heat from the solar field is input to the compressed air in the gas turbine. The comparisons are based on technical and economic performance of the 3 configurations at different solar share. Two analyses were performed; the first considers the conservative technical limits of the power plants equipment, while the second considers the maximum feasible limits. Both analyses were focused on the performance of the plants at different annual solar share. Energy system modelling was utilized in this study and not power plant modelling, where fewer details are considered.

  In comparison to the work of this thesis, No comparison was performed with PV-CSP hybrid plants, no power plant optimizations were performed to obtain the optimum power plant for each technology, and finally the study was based on energy system modelling, so detailed power plant design and dynamic performance were not considered in this study.

- **HYBRID PHOTOVOLTAIC POWER PLANTS: LEAST COST POWER OPTION FOR THE MENA REGION**, by Christian Beyer and J. Reib, 2010

  This study analyzed the performance of hybrid plants based on 24 different configurations of the following technologies: PV, wind, CCGT, CCGT with CCS, conventional coal, coal with CCS and renewable power methane (producing hydrogen from RE and then combining hydrogen with Carbon dioxide to produce methane). No optimization was performed in this study, and the hybridized plant that would be relevant is the PV-Wind-CCGT, which is still different than what is discussed in this thesis.

- Many efforts were exerted within the KTH solar research group in developing CSP and PV-CSP hybrid plants, which will be utilized in this study to be benchmarked with the PV-CCGT model at a specific unprecedented location.

1.2. Objective of the Study

The objective of this work is to study the competitiveness of CSP and PV-CSP hybrid power plants in utility scale application for power generation purposes and to compare it to hybridized combined cycle gas turbine (CCGT) with PV. This study is to be carried out for a location in the MENA region, designated, the UAE. In order to carry out this comparative analysis, a techno-economic analysis is to be done for each of the mentioned technologies (CSP, PV-CSP and PV-CCGT) and to identify the optimum configuration of each technology then compare the techno-economic indicators of each technology considering that technical requirements are met and that the comparison between the three plants is consistent.

A breakdown structure of this objective could be summarized in the following points:

- Developing a model of the PV-CCGT, in terms of dynamic performance and financial model.
- Creating the needed data for a new location (UAE), such as weather data, technologies cost related data, and financial related data….etc.
- Customizing the existing CSP and PV-CSP models on the new location.
- Running multi objective optimizations (MOO) for each of the technologies to obtain the optimum plant configuration of each technology.
- Performing comparative analysis between the results of each of the MOOs.

1.3. Methodology

The techno-economic analysis of CSP, PV-CSP and PV-CCGT power plants will be performed by DYESOPT, an in-house tool developed in KTH, which runs techno-economic performance evaluation of power plants through multi-objective optimization for specific locations. For this study, the UAE was chosen for simulating the performance of the plants.

CSP and PV-CSP models (previously developed by the Solar research group in KTH) were customized to the location selected, while a PV-CCGT model has been newly developed for the sake of this study. A multi objective optimization is performed for the 3 models to obtain the optimum plant configuration for each technology; afterwards a comparative analysis was performed. Finally, sensitivity analyses were performed to account for the possible variations of some technical and economic factors, the results are again discussed and a final conclusion is drawn with the possible opportunities of the studied technologies for the UAE and possibly countries in the MENA with similar conditions.

2. Technologies involved in this work

In this section, the different technologies involved in this study will be briefly explained in terms of different types, theory of operation, and some other aspects. These technologies are used in many applications such as electricity generation, desalination, process heat, and solar fuels[13]. The technologies are considered for utility scale electricity generation application (MW scale per unit).

2.1. Concentrating Solar Power

This technology operates on direct sunlight, which is direct beam radiation that is not deviated by clouds and aerosols in the atmosphere and reaches the earth's surface as parallel beams for concentration [12]. The DNI quality is more important for CSP than other solar technologies as PV and CPV, as a CSP plant parasitic consumption and thermal losses are constant, accordingly below a certain level of DNI the net output of the plant is zero [14]. In order for CSP plants to function properly and be economically viable, the DNI of the location should be at least 2000 kWh per square meter per annum [15].

The concept of this technology is based on using mirrors for concentrating direct normal radiation (beam radiation) on a receiver, reaching a temperature range of 400 °C to 1000 °C [12]. The higher the concentration ratio, the higher the receiver temperature and eventually the higher temperature achieved by the power cycle. The receiver is cooled down and the heat energy gained is transferred by means of a heat transfer fluid (HTF). The heat is then utilized for running a Rankine cycle, generating electricity. In some cases, thermal storage facilities are added where the thermal energy from the HTF is stored during the availability of excess energy or off-load hours. There are different types of commercial CSP technologies that have been developed for MW-utility scale electricity generation. Mainly, there are four main types: Parabolic troughs and linear Fresnel systems, which are line-concentrating shown in figure 2, and central receivers (Solar Tower) and Parabolic dishes (with Stirling engines), which are point-concentrating shown in figure 3 [14].

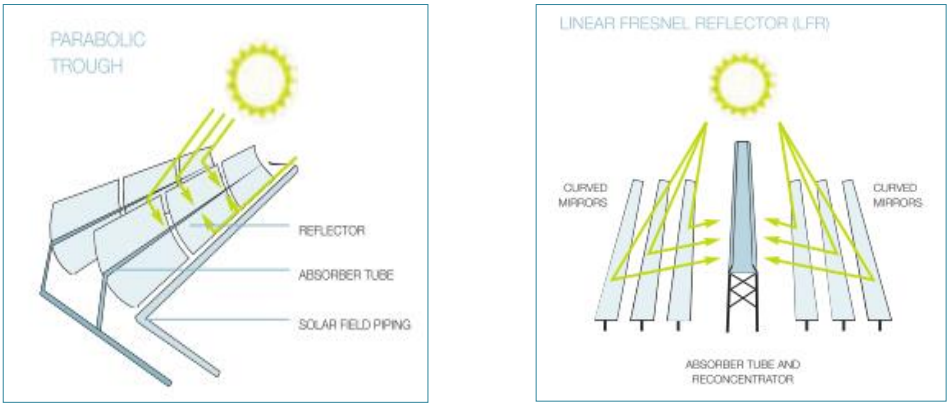

Figure 2. Parabolic Trough and Linear Fresnel System, line concentrating types[12]

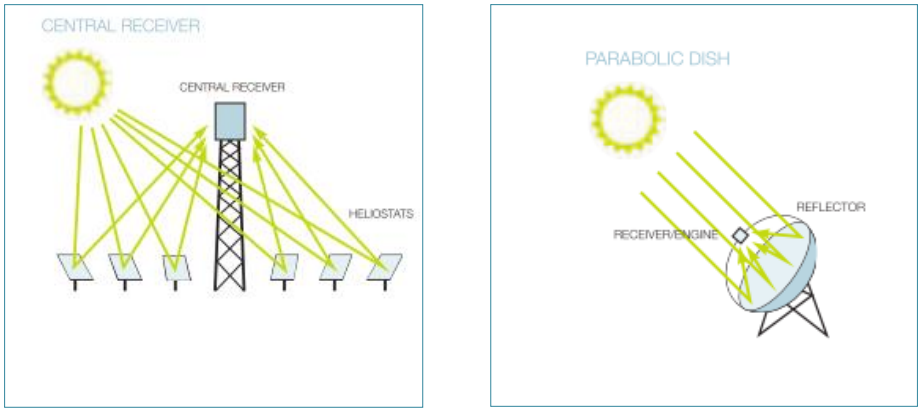

Figure 3. Central Receiver and Parabolic Dish, point-concentrating types [12]

Parabolic dishes will be excluded from this study as it is not convenient for utility scale generation(in terms of generation per unit)[13] and there is no commercial storage solution yet available, and accordingly it will not make sense to compare it to the other 3 technologies in this study. A brief description with advantages and disadvantages of each type (excluding Parabolic dish), will be explained in the following sub-section.

2.1.1. Types of CSP technologies

2.1.1.1. Parabolic Trough

Parabolic Trough technology is the most mature CSP technology available in the market and ranked the first among other CSP technologies in terms of installed capacities. It consists of loops of parabolic trough-shaped mirrors tracking the Sun on a single axis. These mirrors concentrate the direct normal radiation onto a thermally efficient receiver tube with a factor of 60 – 80 [16], where a HTF (usually oil) flow through. The fluid is heated up to 390°C [14] and pumped to a conventional Rankine cycle. The heat from the HTF is exchanged through economizers, evaporators and superheaters to produce superheated steam out of saturated water, and generates electricity through a steam turbine generator. Parabolic trough systems

could be hybridized with a combined cycle and thermal storage facilities could be added as well. Parabolic Trough systems are characterized by a proven annual 14% overall efficiency, being modular, and has a good land-use factor. The main disadvantage so far is the HTF as oils is used which limits the operating temperature to only 400°C and the fact that it is flammable [13].

2.1.1.2. Linear Fresnel Systems

Linear Fresnel systems are similar to the Parabolic trough systems, but a series of long flat or slightly curved mirrors are used instead of the parabolic trough-shaped ones. These long mirrors are set at different angles at each side of the receiver, which is located at a higher elevation of several meters above the mirror plane. The mirrors concentrate the sunlight onto the receiver with a factor of about 60. Unlike the parabolic mirrors, in the Fresnel collectors the focal line is somewhat distorted, accordingly a mirror is required above the receiver acting as a secondary reflector to refocus the rays missing the receiver. A wider receiver might be used, which consists of multiple tubes that are wide enough to receive all the reflected rays. The operating temperature of this technology reaches 350°C [15]. The main advantages of this technology are low cost and high land-use efficiency, while the disadvantages are low operating temperatures and only small projects of this technology are operating [13].

2.1.1.3. Solar Tower Power Plants (Central Receiver)

Solar Tower technology is a point-concentrating type where large mirrors with tracking (Heliostats) are used to focus sunlight on a central receiver on a top of a tower, with a concentration factor of 600 – 1000 [17]. Through this central receiver, a HTF circulates to extract the heat energy gained from the highly concentrated radiations by the heliostats to generate superheated steam in a conventional steam cycle and generate electricity through a steam turbine generator. The HTF could be water/steam, molten salts, liquid sodium and air. High temperatures are achieved by this technology, reaching 1000 °C when air is used as a HTF[13]. In case of using air as a HTF the solar field is integrated with a gas turbine, or a combined cycle with a topping gas turbine. This technology is characterized with high conversion efficiencies and integration with storage and storing energy at high temperature.

2.1.2. CSP Technologies market overview

According to CSP today 2014 Solar tower report[18], solar tower technology is expected to play an important role in terms of capacity share and market activity. As detected by “CSP today” global tracker (July 2016), the data in table 1 shows that parabolic trough technology is by far the top in terms of “capacities in operation” and “construction”, yet, solar tower technology, represents more than 65% of total capacities in planning and development

phases [19]. This means that the eyes of the industry are highly focused on this technology, in addition to the claims that this technology is the most viable route towards grid-parity.

	Planning	Development	Construction	Commissioning	Operation
PT	2095	1021	1722	0	4182
CR	6012	1018	643	6	661
Fresnel	131	174	135	0	175
Dish	150	33	0	1	1.22

Table 1. Status of Global capacities (MW) for each technology (Status that were excluded: Announced, Cancelled, On hold, unconfirmed)

Another study showing the results in figure 4, where solar tower technology (CR) has the lowest LCOE, compared to PT and LF. Fresnel technology is the cheapest in terms of investments but the production is quite low compared to CR and PT which is obvious from the capacity factor indicator, that is why it resulted in the highest LCOE [20].

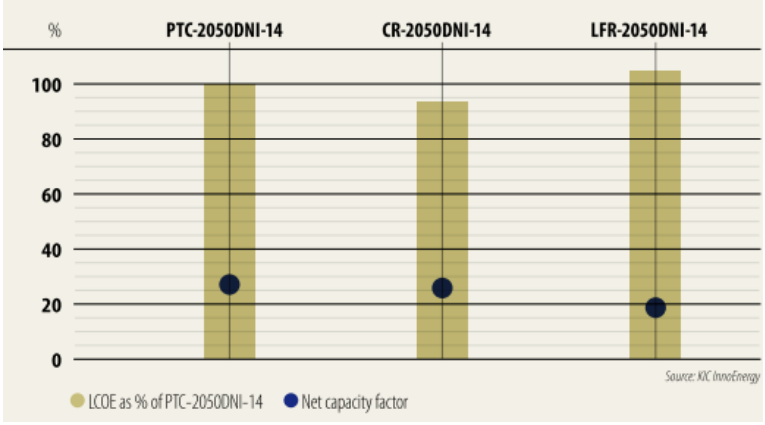

Figure 4. Relative LCOE and net CF for central receiver (CR), parabolic trough (PT), and Linear Fresnel Reflectors (LF)[20]

2.1.3. CSP technology of choice

From this stand point, the solar tower technology was chosen to be the technology of choice in this study, among the CSP available technologies. Thermal storage facility will be included in the selected model for lowering the LCOE and achieving dispatchability, accordingly direct steam generation model of power plants is excluded, and finally the chosen model is solar tower system with molten salts as HTF, thermal storage facility of 2 tanks with molten salts (the most proven technology) and a conventional steam cycle as a power block.

2.1.4. CSP in details with focus on Solar Tower technology

As shown in figure 5, there are 3 main blocks that build the solar tower power plant: Solar field, Thermal Energy Storage block (TES), and the Power Block. The solar field is the block

harnessing thermal energy from solar radiations and transferring it to the HTF (Molten salts in this case), the TES block is where the excess thermal energy stored in molten salt tanks and discharged according to requirements, and finally the power block where the heat energy is converted to electricity through exchanging heat with the power cycle (water/steam in this case) and electricity is generated through a steam turbine generator. In the following section a brief description will be explained for each key component of the plant.

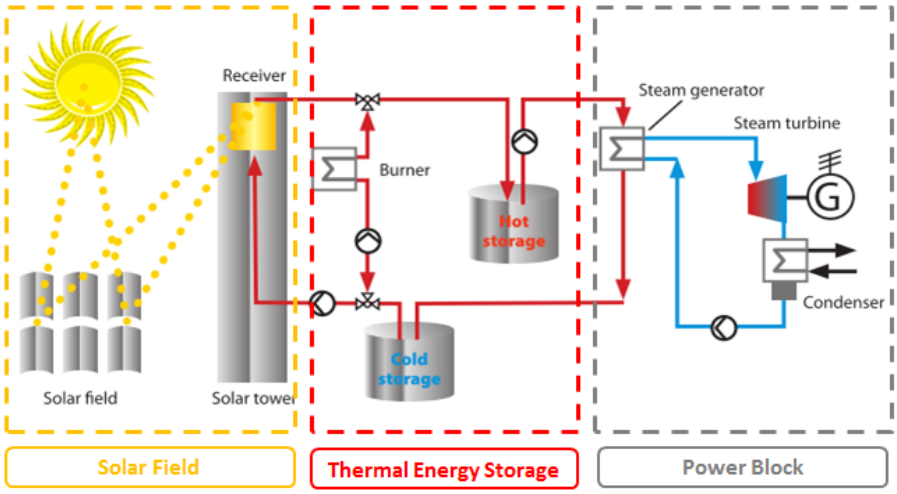

Figure 5. the three main blocks of a solar tower power plant[18]

2.1.4.1. Solar Field

The solar field (SF) is the most CapEx intensive block in the CSP plant, the 2 main components of this block are the Heliostats and the receiver.

2.1.4.1.1 Heliostats

Heliostats are an essential component in the STPP, and the most expensive component in the cost structure of this technology. Heliostats are dual-axis tracking mirrors, reflecting DNI onto the central tower receiver located 100 to 1000 meters away. Mirrors on heliostats are almost flat; a slight curvature is required for better focus. Normally, large heliostats consists of smaller mirrors assembled on a substrate backing as shown in figure 6, the concave surface is formed by tilting the smaller mirrors toward a point on the receiver, so that the focal length of the heliostat is the distance between the receiver and the furthest heliostat [18]. There are no standard dimensions of heliostats, their sizes vary in a range from 1 m^2 to 160 m^2[14]. Different designs of solar fields are possible where the heliostats are arranged in different patterns taking into consideration shading, blocking, and attenuation at further distances from the central tower.

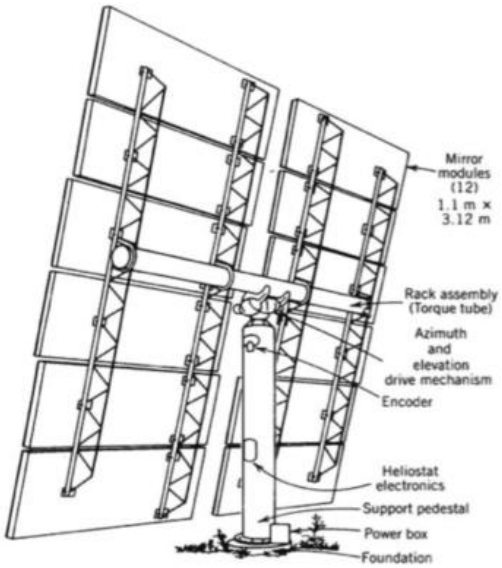

Figure 6. Back view of a Heliostat unit[18]

2.1.4.1.2 Receiver

The receiver is placed over a tower in order to receive the reflected radiations more efficiently. Towers are usually made with steel structure or concrete, through analysis it is proven that at heights below 120 m steel is more economic and more than 120 m, concrete is less costly. Receivers could be classified to external and cavity receivers, external receivers are formed of vertical pipes welded together forming a cylindrical shape where the HTF passes through those tubes to heated to the desirable temperature, while the cavity type serves for reducing the convective losses from the receiver where the absorbing surfaces are located inside cavities at the top of the tower. The two types are shown in figure 7 (a) and (b) respectively.

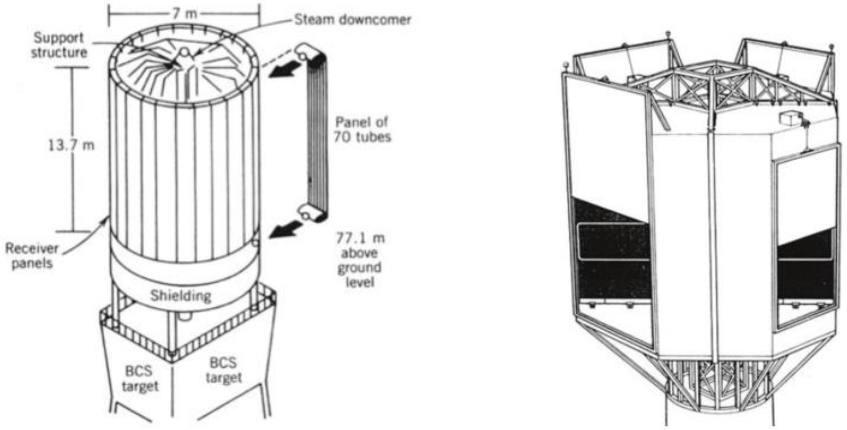

Figure 7. (a) External-type receiver. (b) Cavity-type receiver with 4 apertures[18]

2.1.4.1.3 Solar Multiple

The solar multiple is defined as the ratio between the solar field thermal power at design point to the power block thermal power at nominal conditions, as shown in equation (1), where $\dot{Q}_{SF,thermal}$ is the thermal power from the solar field while $\dot{Q}_{PB,thermal}$ is the thermal power required by the power block. It simply compares the solar field size to that of the power block, in terms of thermal power.[21] This parameter ranges between 1.1 and 1.5 (reaches 2 for Linear Fresnel Reflector) for plants without thermal energy storage, while those with thermal storage may have a value from almost 3 to 5.[17] This parameter is always higher than 1 in order to achieve the power block nominal conditions for a longer interval. As shown in figure 8 the difference in terms of "nominal performance interval" is quite clear between 2 plants of SM 1 and 1.5, on the other hand the spillage or the energy lost is much higher in case of the plant with SM of 1.5 (considering no TES). Plants with higher solar multiples have relatively higher LCOE due to the non-profitable solar field installed.[21]

$$SM = \frac{\dot{Q}_{SF,thermal}}{\dot{Q}_{PB,thermal}}\Bigg|_{at\ design\ point} \quad (1)$$

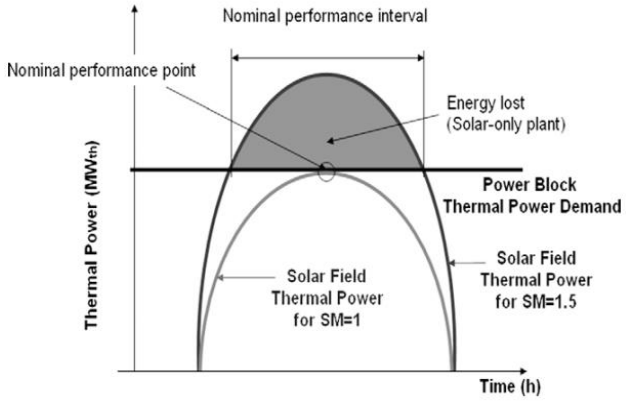

Figure 8. Daily thermal power for CSP plants with different solar multiple [21]

2.1.4.2. Thermal Energy Storage (TES)

The thermal energy storage technology utilized in this study is "Two-Tank Direct System", which involves the fluid collecting solar energy to be the same as the one used for energy storage, which is molten salts in this case. The system comprises of two tanks at two different temperatures, low and high temperature. During charging, the fluid flows from the low temperature tank (cold tank) to the solar receiver, and then stored in the high temperature tank (hot tank). In hours with insufficient irradiance, discharge takes place where the fluid flows from the high temperature tank (hot tank) to the power block heat exchanger, generating steam, and stored afterwards in the low temperature tank (cold tank). [18]

Integration with thermal Energy Storage (TES) is an advantage that makes CSP a favored option among other renewable energy technologies, where it provides an economic feasible solution for energy storage. The advantages are that it allows the plant dispatchability, which is the ability to provide electricity on demand [13], in addition to being decoupled from the availability and intermittency of the solar resource. In terms of short interval energy storage, it smooths out the electricity production as it works as a buffering reserve, while in long interval storage (several hours), the CSP plant could reach high capacity factors and follow the demand curve without any dependence on the solar input availability.[13]

Figure 9 shows the output of different technologies, Photovoltaic and CSP with direct steam generation (DSG) does not incorporate any storage facility and accordingly those technologies follow the solar input, while in case of CSP with storage shown in green and yellow, firm power output and dispatchability are achieved.[22]

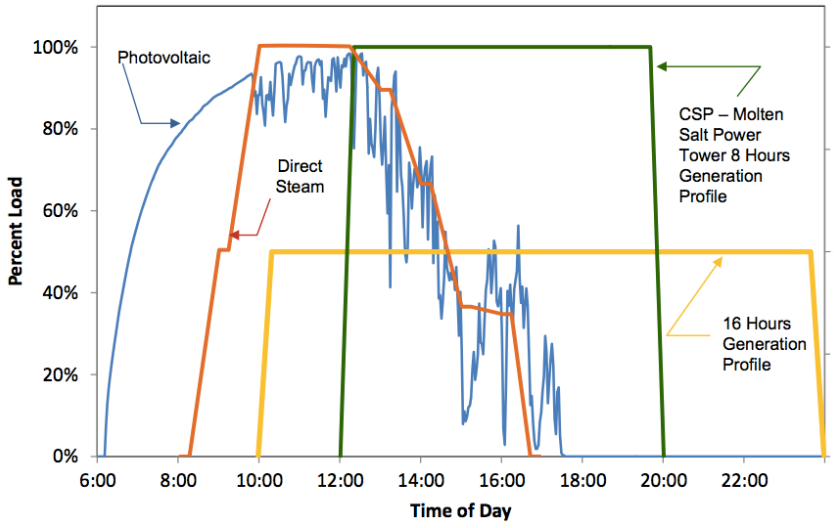

Figure 9. Dispatchabilty of CSP with TES compared to other technologies[22]

2.1.4.3. Power Block

The power block in this application is basically a steam cycle, where the heat exchanger replaces the heat recovery steam generator (HRSG) and the rest of the cycle is nearly the exact same, where superheated steam is expanded in different turbine stages, with reheat in between, and steam bleeds for preheating the feedwater entering the heat exchanger. The difference lies in the special operation mode of such steam turbines, unlike normal combined cycle plants and Steam cycles were the steady operation at rated power is the common mode of operation, the steam cycle associated with the CSP plants requires more flexibility and higher efficiencies at partial loads as this is the normal mode of operation in this application[18].

2.2. Photovoltaic (PV) solar panels

PV systems are basically solar modules that are commonly either c-Si (crystalline silicon) or of the thin-film type. Crystalline silicon materials incorporate monocrystalline and polycrystalline types, while thin film technology has many semiconductor materials including Cadmium Telluride (CdTe), Copper Indium Gallium Selenide (CIGS), and amorphous Silicon (a-Si). Thin film technology is always cheaper as the involved materials are less expensive to produce, and characterized by lower conversion efficiencies. Many thin-film materials have been introduced, yet the aggressive reduction in c-Si modules has vanquished the cost advantage of the thin-film technology[23]. The solar modules directly convert solar energy into electricity through Photo-Voltaic effect. Direct current electricity (DC) is produced which requires an extra component for conversion to alternating current electricity (AC), which is the inverter.

In the last years, PV has reached an amount of annual installed capacities that is unprecedented. Many reasons are behind this achievement, but the most important is the rapid decline in solar module prices[23]. Further details about the technology, market, design and cost, could be found in [24], [25], [26], [27], and [28].

2.3. Combined Cycle Gas Turbine (CCGT)

The principle is based on integrating one or multiple gas turbines with a steam power plant where the heat source of the steam power plant is the cold source of the gas turbine(s). The heat from the exhaust gas of the gas turbine is recovered by means of heat recovery steam generator (HRSG), generating superheated steam for expansion in a condensing turbine. The output is the most efficient fossil fuel to electricity converter. Thermal efficiency exceeds 55%, with the gas turbine providing two thirds of the total capacity and exhaust gases could be exceeding 550 C. The remaining third is provided by the steam turbine, which is fed by superheated steam at 85-100 bars and 510-540 C.[29]

Combined cycles built in the 1990s and the early 2000s were typically designed for base load operation. Due to the increased contribution of non-dispatchable renewable energy generation and the overcapacity in a liberalized market, it became very important for combined cycles to operate at part load and be subjected to frequent load changes. Due to these factors, it is common for combined cycle power plants to be shutdown at night and during the weekends as the cost of energy production is less than the revenues in some markets. In addition, due to the high penetration of renewables in some regions, and intermittency being a nature of such kind of generation, grid reliability is compromised. Accordingly high flexibility, efficient partial load operation and reduced minimum operation load, became crucial features for combined cycles. Partial load operation is generally characterized by efficiency reduction relative to full load operation. It is generally due to the

decrease in the gas turbine efficiency, which is accounted for the lower pressure ratio and firing temperature at partial load. Modular configurations of 2 gas turbines on 1 steam turbine improves the total gas turbines efficiency at partial loads, in addition to the operation at a lower minimum load, as the minimum load for operating 1 gas turbine is half the minimum load of operating both compared to the total power as one could be shutdown. [30]

The technical minimum environmental load is a very important term that should be identified. It is defined as the minimum possible load that the gas turbine can operate on, keeping the NOx and CO emissions within the environmental limits. The minimum load of GT operation is more impacted by the NOx rather than the CO emissions.[31]

A lot of research and development is dedicated to reduce the minimum load of operation of a GT in order to be able to operate the GT at a wider range of loading, accordingly it is easier for the whole plant (CC) to follow the daily load profile variations and the intermittency of solar PV generation, in case of PV hybridization. According to a report issued by IEAGHG in June 2012 the technical minimum load of a gas turbine would range from 30% to 50% of full load of the gas turbine [31]. While another report issued by Alstom in 2011 describing the low load operation of the KA26 combined cycle, it was stated that the minimum load at which a combined cycle power plant (equipped with GT26 with sequential combustion)could operate, complying with emission limits could reach below 20 % [32].

Recent combined cycle power plants are well developed for meeting current market requirements in terms of fast response (ramping up and down), quick start up low load operation reaching 14% of plant base load while maintaining emissions constraints [33]. From [32] and [31], it was concluded that the operation of the GT at 10% of baseload is technically possible and accordingly this was the operation limit assumed in this study in order to allow maximum possible integration of PV and minimum curtailment.

This flexibility comes with some drawbacks such as the low fuel efficiency during operation at part load, compared to that during base load operation, as well as higher rates of NOx and CO emissions. The good news is that the effect of renewable energy penetration overcome both of the formerly mentioned drawbacks.[34]

Due to the increase in the rate of installed capacities of renewable energy generation added every year[34], OEMs tend to improve those functions by several initiatives, such as: 1) Full dispatchability between the HRSG and the Gas turbine, to allow the GT from ramping up without impacting the HRSG. 2) Several solutions for heat retention during shutdown to reduce heat losses during shutdown and achieve a quicker start. 3) Implement high degree of automated and reliable start-up for the plant. 4) Implement highly complex control systems capable of providing convenient ramp rates for each component according to its state.[35]

2.3.1. Heat Recovery Steam Generator (HRSG)

The HRSG is a main component in a combined cycle (CC) which acts as a heat exchanger between the exhaust gases of the gas turbine and the saturated water fed by the feed-water pumps. The HRSG requires slow heating rates due to the thick walls of steam drums, while in case of once through HRSG (Benson-type), there are no steam drums, so no manifolds/containers with thick walls which allows quick start of the gas turbine and the once through HRSG is the recommended type for CC used in cyclic applications [35].

2.3.2. Steam turbine

Another critical component in the CC , which received a great contribution of innovations and improvements to reduce the startup time as the ones mentioned above. These improvements allowed the CC to start and respond much faster, specifically during hot starts and load-following mode [35]. Although higher configurations of combination of gas and steam turbines would allow lower operation load and higher efficiency, yet higher configurations might require a larger steam turbine which has a higher start-up time and the flexibility known for combined cycles might be harnessed and it will be more convenient for base load operation (large capacities). [35]

2.4. Hybridization

2.4.1. PV-CSP

Operational hybridization of PV-CSP is the concern of many research studies and has been implemented recently in projects as Atacama-1 in Chile developed by Abengoa [36], and Copiapó in Chile as well, developed by SolarReserve [37] and others. The hybridization is based on the prioritization of the PV plant o/p whenever available, while the remaining capacity is complemented by the CSP plant which provides dispatchability for the whole complex due to the integration with a TES facility, and it can dispatch with response to the PV plant output. As shown from the plant layout in figure 10, the hybridization is performed on the operational level, where both plants together provide a specific required firm output by means of smart dispatch control. The main advantage of this hybridization is the reduction of the LCOE of the whole plant compared to only CSP, in addition to achieving higher CF for the same LCOE when compared to CSP alone.

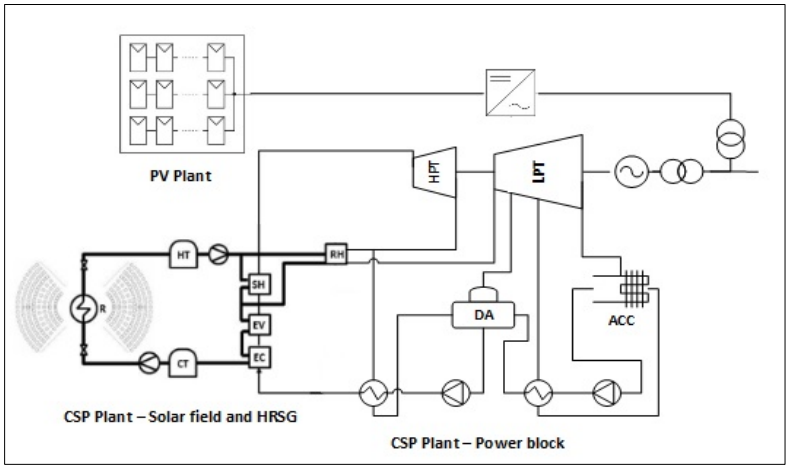

Figure 10. PV-CSP plant layout

2.4.2. PV-CCGT

The hybridization of PV-CCGT is performed on operational level as well, same as in the CSP case, whenever PV production is available, it is prioritized and the CCGT plant ramps down in order to accommodate the PV production, while the whole plant provides a required specific firm output by means of smart dispatch control. The PV-CCGT plant layout is shown in figure 11. The advantage of this hybridization is the reduction of carbon emissions generated from the CCGT, in addition to the reduction of OpEx, as less fuel is burnt with higher PV integration. This concept is not implemented yet, but it is analogous to having both technologies: PV and CCGT, as generators in a certain grid where the plants operation is managed on the grid level. PV capacities are recruited when available and Gas turbines as well as CCGT are recruited to cover the demand unmet by the renewable intermittent generators and the relatively fast response, especially for GT is the advantage that allows this functionality.

The advantage of having the hybridization on the plant level is depicted in the simplification in control and providing the possibility of sharing electrical inter- connection lines and infrastructure in order to reduce costs.[2]

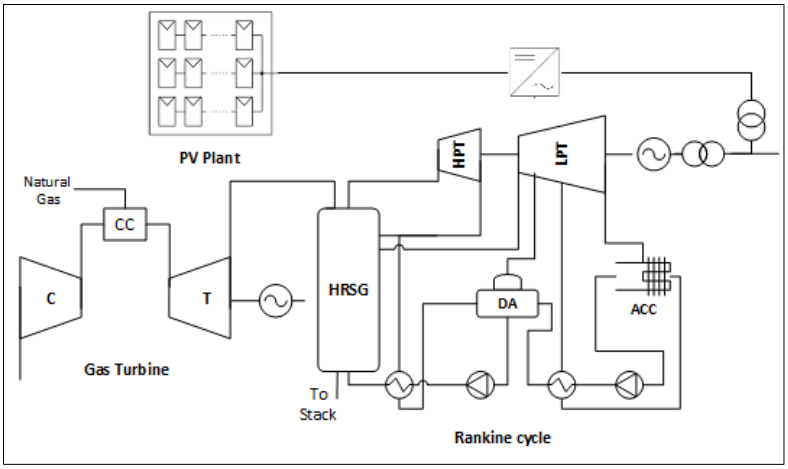

Figure 11. PV-CCGT plant layout

3. The MENA region

Across the MENA region almost all the countries of the region are endowed with an average to high solar resource, as shown in figure 12, extracted from IRENA solar atlas [38], the GHI in the region reaches more than 2600 kWh/m^2. In order to choose the location of this study, many factors have been considered in accordance with the technologies under study. The criteria of the chosen location was essentially the solar resource, natural gas resources (where the gas fired combined cycles will still be attractive), land resource (as CSP and PV require vast land areas), policies and legislations promoting renewable energy and carbon emissions abatement, previous similar successful projects and relevant future plans with regards to the technologies under study, and finally a stable political situation that stimulates flow of investments into such projects.

Electricity demand has been rising in the MENA region between 6% and 8% as a mean average growth rate. Some power plants in the GCC countries experienced an increase in peak load with 12% comparing 2014 and 2015 summer loads. Baseline projections for the region show a total yearly energy consumption of 1000 TWh by the year 2020, from only 800 in the year 2012. [39]

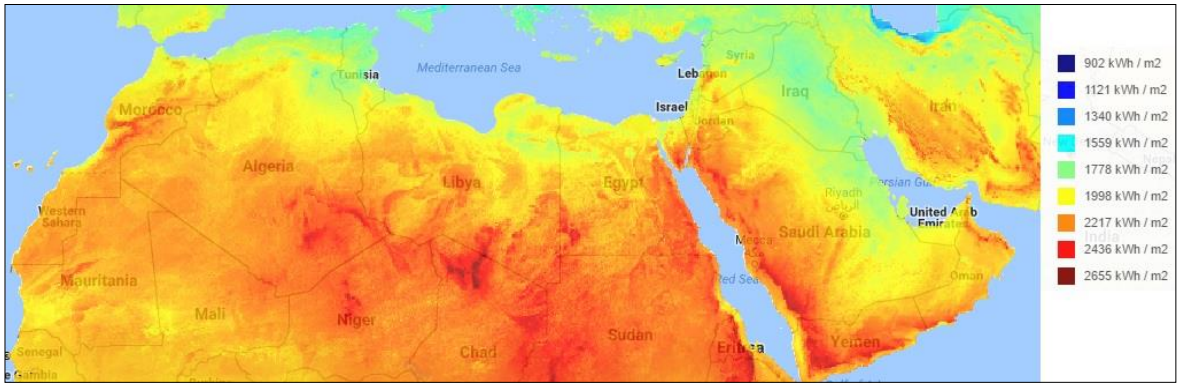

Figure 12. MENA region solar map – HelioClim3 – GHI [38]

4. Country of choice: UAE

The United Arab Emirates (UAE) was the country of choice considering the above mentioned criteria. The country does not score highest in each criterion, but provides a general good compromise. The UAE consists of seven emirates: Abu Dhabi, Dubai, Sharjah, Ras Al Khaimah, Ajman, Umm Al Quwain and Fujairah, covering 83,600 km² of land area with a population of 8.45 million (2012), installed power capacity of 30 GW and electricity consumption of 87 TWh[40]. Abu-Dhabi and Dubai forms the core of the economy of the country[40], and the only emirates involved with renewable energy activities.

4.1. Solar resource

The solar resource is not the highest in the region yet it could be considered as an average. In 2010 the measurements showed DNI were ranging from 1900 to 2200 kWh/m2, while GHI measurements were ranging from 2100 to 2300 kWh/m2 across the country. As shown in both GHI and DNI solar maps in figure 13 (a and b), the Southern parts of the country have the highest irradiation, yet these regions are uninhabited, eventually no transmission lines exist there. The Northern parts have lower values, and the lowest is for the Northeastern coastal region where the concentration of airborne dust particles is at its highest and the humidity from the coast. The dust particles and humidity impact intensively the DNI values and this is obvious from figure 13 (a).[41]

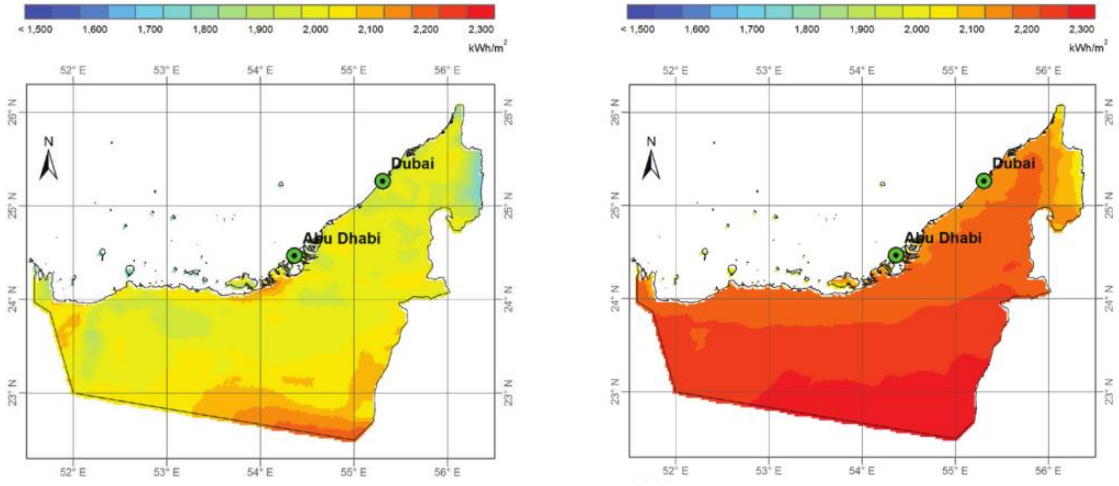

(a) DNI of UAE in year 2010

(b) GHI of UAE in year 2010

Figure 13. DNI (a) and GHI (b) of the UAE in year 2010 [41]

4.2. Natural gas resources

The next criterion is the natural gas resource, where the UAE is considered one of the world largest hydrocarbon reserves holders and exporters. The UAE is ranked seventh in terms of natural gas reserves[11] with 6.1 trillion cubic meters[42]. In terms of production the UAE is ranked the 17th globally, producing 9.4 billion cubic feet per day. Despite the huge production, UAE is a net importer of natural gas due to the immense demand increase in electricity which is almost completely based on natural gas. The gas imports are from Qatar through the Dolphin gas export pipeline connecting Qatar and Oman through the UAE. [42][11][43][40]

4.3. Previous and planned projects

As mentioned earlier Dubai and Abu-Dhabi are the most important emirates in the UAE generally and specifically with regards to renewable energy activities. In this section it will be obvious that all renewable energy projects are taking place either in Dubai or Abu-Dhabi.

Abu-Dhabi:

SHAMS 1 is the first and only so far, CSP plant to be built in Abu-Dhabi. A 100 MW capacity using parabolic troughs technology hybridized with fossil-fired back-up, developed and owned by Masdar, Abengoa and Total [40], [44]. In addition to the 10 MW solar PV plant installed as well, by Masdar city using multi-crystalline and thin film solar panels from Suntech and First Solar [45]. Abu-Dhabi is having its first big PV project in tendering phase, of a 350 MW capacity[39].

Dubai:
Dubai's biggest project is the Mohammed bin Rashid Al Maktoum Solar park. Phase 1 of this project was only 13 MW and was inaugurated in October 2013, owned by DEWA and developed by First Solar [46].On the residential application side, Shams Dubai project was initiated to encourage residential installations of PV, and 4 MW of PV are installed on buildings' rooftops.

In terms of planned projects, the nearest is the 200 MW CSP power plant which is currently under tendering for advisory services [47], which will be operational by 2021 [48]. Another 2 projects in the pipeline are: the phase 2 solar PV of 200 MW of the famous landmark PPA of 5.85 US cents/kWh [39]developed by ACWA power to be operated in 2017 [49], and finally phase 3 of the 800 MW solar PV with the world record of 2.99 US cents/kWh awarded in June 2016 to a Masdar-led consortium including the Spanish companies FRV and GranSolar Group, the 800 MW plant should be operational by 2020 [50]. Mohammed bin Rashid Al Maktoum Solar park is planned to include a capacity of 1000 MW by 2020 and 5000 MW by 2030, where the CSP technology will generate 1000 MW out of the 5000 MW by 2030 [48].

Dubai future plans represents a solar contribution of its energy mix of 25 % by 2030, and renewable contribution to be 7% by 2020, 25% by 2030 and 75% by 2050, while Abu-Dhabi's official clean energy target is still 7% by 2020 [39].

4.4. Land resource

In terms of land resource, the total land area of the UAE is 83,600 Km^2, of which mainland represents 77,700 Km^2[51] compared to other countries in the region, such as Saudi Arabia, Algeria, Egypt, Sudan and others, the UAE is much smaller. Yet the land utilization in the UAE is quite low, for example in Abu Dhabi, only 30 % of the land is inhabited [52], providing plenty of land areas for building power plants with such technologies that consume large land areas.

4.5. Political and economic situation

According to Coface risk assessment of the UAE, politically the country is considered as a safe-haven within the turmoil all over the region since 2011. The business climate is considered the most favorable in the region. Economically, due to the diverse economies of international trade, air transport, tourism, and financial services that contributes up to 44.5% of GDP [53], the country was able to be resilient against the drop in hydrocarbons prices started in 2015 [54]. However, this declination in oil revenues created a budget deficit, which is expected to remain in 2016, but positively pushed the government into the direction of

reform of energy subsidies [54]. Meanwhile the banking sector stays profitable, liquid and well capitalized [54]. Worth mentioning that the UAE was Ranked second, after Saudi Arabia in the EY Cleantech survey report MENA 2014, as the country with the highest potential for renewable energy investments within the next five years[55].

4.6. Case study

In order to proceed with the UAE as a country for the case study a specific location should be selected, as the country consists of seven emirates, each with a dedicated electricity market operating at the emirate level [40]. Although Abu Dhabi was the early adopter and pioneer of the solar technology in the country through the SHAMS 1 plant, in this study, the emirate of Dubai was selected due to the clear announced solar energy related policies extending till the year 2030, with serious steps towards achieving the targets announced.

4.6.1. Projected Energy mix

The electrical power generation in Dubai is basically dominated by natural gas, where all power plants are gas fired of 9.7 GW installed capacity, 7.1 GW of which are gas turbines, 2.5 GW of Steam turbines and a tiny 13 MW solar PV plant as the first phase of the famous solar park previously mentioned [56]. A roadmap has been set by the supreme council of energy (DSCE) aiming for reducing the dependency on natural gas through penetration of 7% clean coal, 7% Nuclear and 25 % solar by 2030, with the remaining 61% as natural gas as shown in figure 14 [57]. Most of the electricity generation power plants are desalination power plants as well, as the country lacks fresh water bodies and depend on fresh water wells and sea water desalination as a source of fresh water.

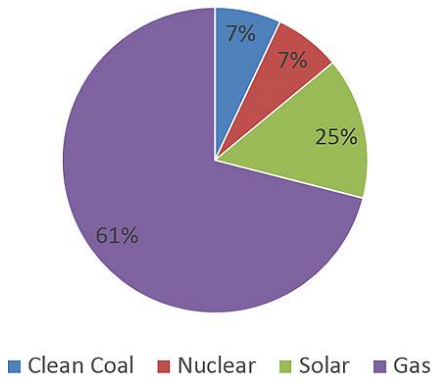

Figure 14. Dubai projected energy mix by 2030 [57]

4.6.2. Typical daily demand profile

The typical daily demand profile of Dubai was concluded from two different profiles, as Dubai's typical daily demand profile was not found through the literature review performed.

The first profile is a typical daily demand profile of a prototypical MENA city with a typical demand pattern and a supply mix of open and combined-cycle turbines, shown in figure 15 below that was used in a study performed by Pwc (Price Waterhouse and Cooper) and ESIA (Emirates Solar Industry Association)[58]. This profile shows a logical steady demand during the night, and a smooth rise starting at 6:00, and ramps faster at 9:00 creating a peak at 12:00 and declines with the same rate to create another small peak at 18:00 and declines again till reaching an almost steady demand during the night. As obvious, those peaks are covered by gas turbines. Solar irradiance levels are perfectly matched with the major peak taking place at 12:00, which makes solar energy an optimum power generation solution for such case.

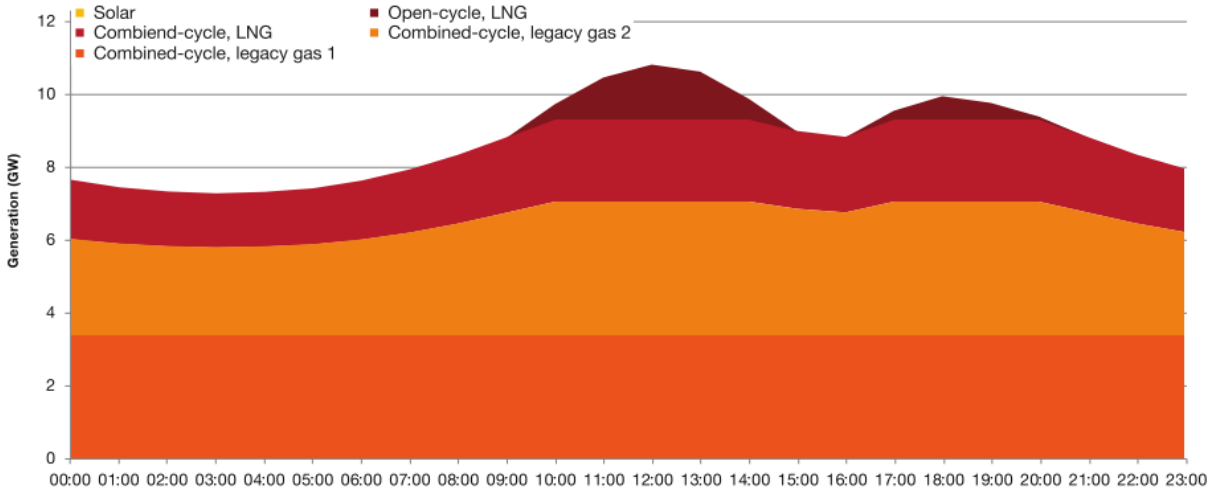

Figure 15. A typical daily demand profile of a typical MENA city [58]

The second profile is Abu-Dhabi's typical daily demand profile for the year 2014 [59], shown in figure 16 below. During winter, the profile shows a minimum demand day with almost a firm demand with a slight rise starting at 4:00 and another rise at 17:00 lasting for about 4-5 hours and then a declination till 4:00 again. The maximum demand variation along the day is about 20% and it is quite smooth without any spiking peaks. During summer and due to high temperatures and humidity the enormous cooling / Air-conditioning load doubles the capacity needed and create some minor deformations to the smooth typical winter day demand profile. At 6:00 - 7:00 the demand profile ramps up to +15% in about 3 hours and along the following 10 hours it remains steady with slight rise during the evening hours 14:00 to 20:00 and finally declines during the night till 6:00. The maximum demand variation along the day is about 23% and still no significant peaking spikes.

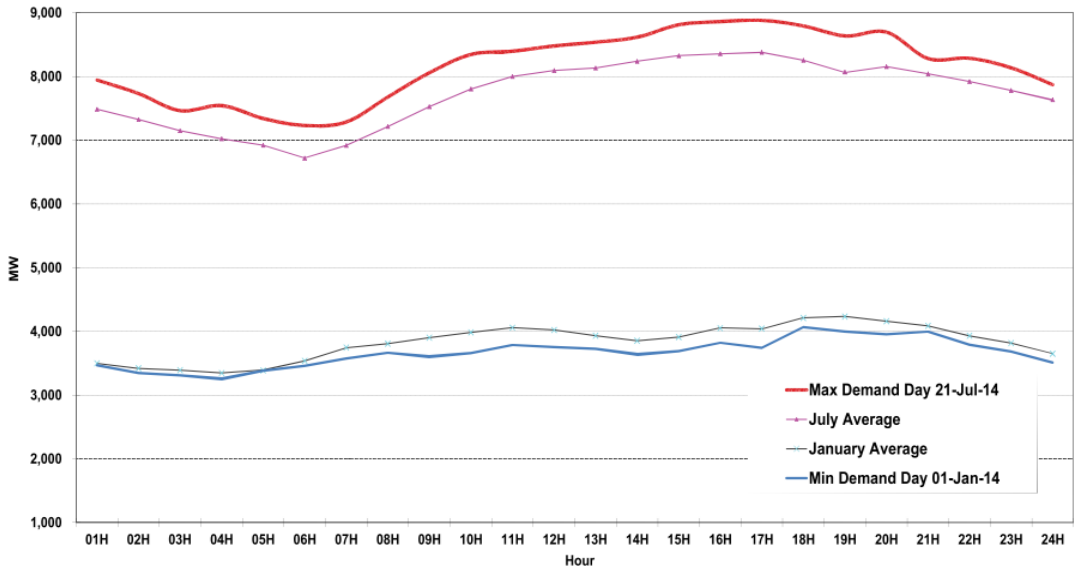

Figure 16. Abu-Dhabi 2014 minimum and maximum daily demand profiles[59]

According to DEWA (Dubai Electricity and Water Authority) website, peak load hours are reported to be from 12:00 to 17:00 [60]. From the former mentioned profiles, the intermediate load (Between peak and base load) for Dubai was assumed to be of 15 hours, from 6:00 to 21:00.

4.6.3. Electricity and water market

In the UAE electricity is always associated with water, this will be obvious in all the governmental entities mentioned in this section, all managing both electricity and water facilities. The electricity and water market was wholly owned by the government in Dubai, where Dubai owns and operates all Power generation and water desalination plants, transmission and distribution networks. Lately private sector participation was encouraged for the economy to continue growing and develop. Accordingly IWPP (Independent Water and Power Producer) model was implemented where a government regulator (Regulatory and Supervisory Bureau for Electricity and Water) license and regulate new entrants to assure that the services provided are safe, reliable and efficient. Another important government agency, is Dubai Supreme Council of Energy DSCE, which is the policy making body of the energy sector, develops strategies, provide governance, and create policy frame-works for Dubai's energy sector assuring diversification of Dubai's energy mix, promoting renewables penetration, and improving energy efficiency. [61][62][40]

The electricity and water market structure in Dubai could be elaborated as shown in figure 17. The Supreme council (represented by DSCE) develops the policy framework to the operator (represented by DEWA). The operator starts tendering for electricity generation and water desalination projects. Developers bid as IWPPs (Independent Water and Power

Producers), IWPPs will be governed by power and water purchase agreements (PWPA) and other agreements related to ownership, financing, operations and maintenance, EPC, and land lease. Bids are based on minimum price proposed through long term PWPA. The off-taker (also represented by DEWA), procures electricity/water from the IWPP based on the agreed upon PWPA. And finally transmission and distribution system operators (which also represented by DEWA) deliver electricity to customers, who pay DEWA their electricity and water bills according to the set tariffs. The DEWA transmission network is connected to the emirates national grid (ENG) of which DEWA owns 30%. The ENG is in turn connected to the GCC grid. All blocks (activities) colored in green are represented by DEWA, Government agencies in grey, IWPP in yellow/green as DEWA owns equity in the IWPP and finally the customers in orange.[61][40][62]

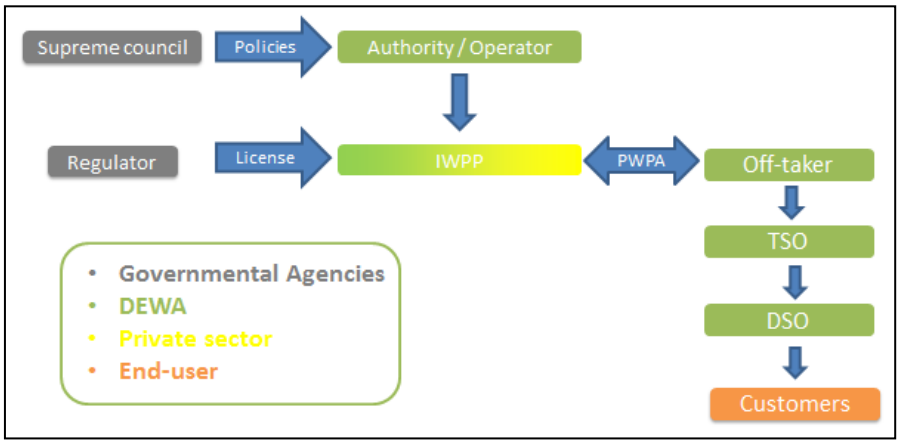

Figure 17. Dubai Electricity and Water market structure

4.6.4. Tariff schemes

Electricity and water tariff schemes in Dubai are all in flat rates depending on the consumption per month, without any variations in peaking hours. This will be directly reflected on a simple, straight forward dispatch strategy.[63]

4.6.5. Previous utility scale solar tenders in Dubai

In 2012, the first phase of the “Mohammad Bin Radshid Al-Maktoum Solar Park” of a 13 MW (DC) capacity was awarded to First Solar as EPC. The project was implemented by DSCE, and is managed and operated by DEWA. O&M services was provided by First Solar as well.[64]

In 2015, Shuaa 1 project, the second phase of the solar park, of 200 MW capacity. The tender was awarded to the Saudi ACWA power and the Spanish TSK on IPP model based on minimum PPA which was a world record at that time of 5.84 US cents/kW. The contract is

PPA-BOT (Build, Operate, and transfer) for 25 years. Shuaa Energy 1 Company was formed as a special purpose vehicle (SPV), with DEWA as 51% stakeholder, and the remaining 49% for both ACWA and TSK. The plant will be operational by April 2017. [65][66]

Recently, in June 2016 the awarding of the 3rd stage of the solar park with 800 MW capacity was announced. The project is an IPP model and the tender was based on minimum PPA provided. The awarding was to a Masdar-led consortium, including the Spanish FRV and GranSolar group, setting a new world record 2.99 US cents/kWh beating the previous record also achieved in Dubai in 2015 of 5.84 UScents/kWh. The plant is planned to be operational in 2020 [67]

The latest tender so far is a CSP project of 200 MW in the “Mohammad Bin Radshid Al-Maktoum Solar Park”. The tender is for advisory services and no further announcements are available.

5. Modelling

DYESOPT (Dynamic Energy System OPTimizer) is an energy system modelling tool that has been created in KTH and is being developed in the solar research department at KTH. This tool so far is based on Matlab and TRNSYS, where MATLAB is used for all calculations within the steady state design, while TRNSYS is utilized to handle the system transients and the dynamic annual simulation of the system. The modelling process goes on by exchanging outputs from one layer to the other as shown in the flow chart in figure 18.[1], [68], [69]

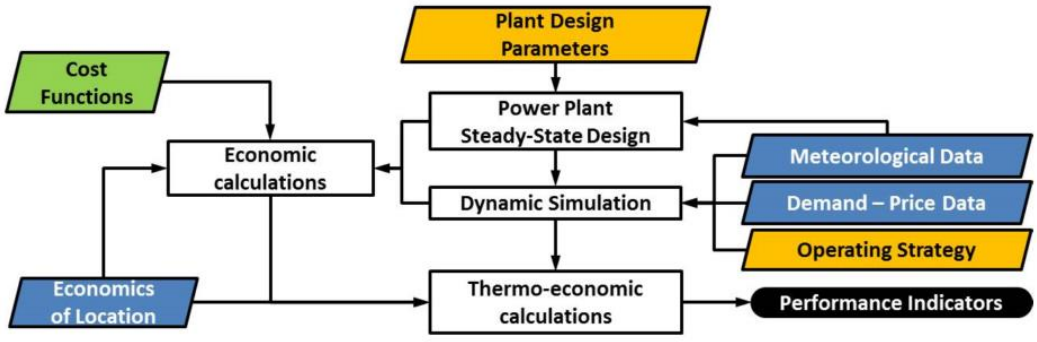

Figure 18. DYESOPT flow chart[68]

In order to elaborate in details how the flow of calculations works, each block of the above mentioned flow chart will be explained and then the interconnections, the system of equations and the flow of inputs and outputs (the process) will be explained in details.

5.1. Steady state design

In steady state design the different blocks of each power plant technology are designed according to specific design points that are input to the model by the user according to the case requirements.

1. CSP-STTP model

The CSP model could be broke down into 3 main blocks: Power Block, Solar Field, and Thermal Energy Storage (TES).

Power block:
The sequence of calculation for the whole CSP model starts from the power block. The steam side is calculated first according to the rated capacity of the CSP plant, which is represented by the rated capacity of the power block, through an iterative process, starting with an assumed steam mass flow rate and ending by checking the power output, till the design mass flow is reached. Through the assumption of the mass flow and the power output check, pressures, temperatures, enthalpies and fluid properties are calculated at each thermodynamic state, considering some input design parameters that are input by the user. Accordingly components are designed where efficiency and flow rates of turbines, heat transfer coefficients of steam train components, temperatures and pressures of the condenser…etc., are calculated.

When temperatures, pressures, enthalpies and fluid properties at each thermodynamic state on the steam train are identified, it is possible to calculate the corresponding points on the heat transfer fluid (HTF) side. Similar to the steam cycle calculation, the HTF cycle is calculated through an iterative process, where the mass flow rate is assumed and check is done across heat balances on the superheater and the reheater. The calculation of the power block is based on previous work by Bergman et al, 2011, and Staine, 1995 [70], [71], while the design of HTF cycle is based on work by NREL, 2008 [72]. [1], [68]

Solar field
The HTF represents the link between the power block and the solar field. Now, the amount of heat energy needed for the power block is calculated, it will be used to solve the solar field. The algorithm for designing the solar field is based on that of DELSOL developed by Kistler[73], it is a hybrid method involving two other methods (handling performance based location and needed spacing to avoid shadowing): 1) Field growth method: At which the field area is evaluated and then the best place for a heliostat is selected, followed by the same process for the second best location, iteration is done till the required heat capacity is achieved. The field area is then divided into zones and the average performance of each zone is evaluated. 2) Optimal radial-stagger pattern method: At which the heliostats are

placed in a radial-stagger pattern to make sure that radial distances and spacing between the heliostats are achieved to avoid any shadowing. A perfectly optimized pattern, doesn't assure a perfectly performing field. Hybridizing both methods provides better results. [1], [68]

Thermal Energy Storage

After the design of the solar field and the power block, it is easy to calculate the storage by knowing the temperature of the HTF, the storage discharge time (size in hrs) (both from the default parameters), and the heat demand required (calculated previously from the power block and solar field). The density of the HTF is deduced through correlations with temperatures. The mass flow rate is deduced from the amount of heat required and the storage size. Using the mass flow rate, time and density, the volumes of the tanks are calculated.

2. PV model

The PV model is developed completely in matlab, even the plant output at each time step. First, the design parameters are input in the tool including the specifications of the PV module and the inverter and many other parameters as the system total capacity (Wp). Then the number of modules in series and the number of strings in parallel are calculated based on the max. allowable voltage (PV module specifications) and the max allowable current (inverter specification). The maximum and minimum values of voltage and current are identified at the hourly global irradiance and temperature values, considering their effects on the nominal values.

After the number of panels is defined as well as the configuration of series and parallel panels, the power plant is considered sized. The next step is to simulate the performance of the plant during the whole year, which is done using TRNSYS in most of the DYESOPT blocks. In this case it is performed in Matlab and the result is a text file with the hourly values ready for import to TRNSYS for hybridization with other models. In order to get these values the solar position should be calculated in addition to the corresponding global irradiance on a tilted surface with the given tilt angle or other, depending on the tracking system selected. The final output of the system is identified before and after the inverter as DC and AC power considering the conversion efficiency of the inverter. Higher values of DC production is curtailed if it exceeds the rated power of the inverter. The final calculated hourly output power is then aggregated to define the annual power output of the plant.

3. CCGT model

A brief explanation of the calculations flow of the CCGT model will be explained in this section. Further details of the model could be found in [74] were the model was created. The steady state of the CCGT model is comprised of two separate models: Gas Turbine (GT) and Rankine Bottoming cycle.

Gas Turbine

First of all, inlet air conditions are identified through input parameters and a built-in fluid properties library, Afterwards the compressor efficiency is calculated through an iterative method where compressor polytropic efficiency, nominal compression ratio and air properties are used. Finally compressor exit air properties are calculated. Fuel properties are calculated in order to model the combustion process. The gas properties exiting the combustion chamber are calculated in order to define the conditions before the turbine.

In the turbine section after the gas composition is identified and the thermodynamic properties of the gas exiting the combustion chamber is identified, the turbine inlet conditions should be calculated as the properties are different due to the cooling taking place in the turbine. So first of all the turbine cooling is calculated in terms of difference of cooling air enthalpy and then the turbine inlet temperature and other conditions are deduced.

The turbine pressure ratio is calculated referenced to atmospheric pressure, followed by the turbine efficiency calculation in order to calculate the enthalpy of exhaust gas exiting the turbine and the rest of the thermodynamic conditions are concluded. Specific turbine and compressor power are calculated, as well as nominal mass flow rate according to the nominal plant (GT) output specified in the input parameters. Finally total net output power is calculated considering the mechanical and electrical efficiencies.

Rankine Bottoming Cycle

The steady state design of the dual pressure Rankine bottoming cycle starts with the design of the heat recovery steam generator (HRSG), where the input to the HRSG is the exhaust gas from the turbine with the previously calculated conditions. Through the design of the thermodynamic status of all points on both sides (gas and steam), the inlet and exit of each of the steam train: economizers, evaporators and superheaters for low and high pressure are determined. Mass flow rate of steam is then calculated through energy balance on the evaporators of each pressure level.

Following the design of the HRSG, that of the turbine is performed, where steam turbines' efficiencies, enthalpies and other properties at inlet and outlet, and output power for each

turbine, are calculated. Finally, condensing system is calculated, determining all parasitic loads in the cycle and accordingly the net output power is deduced.

5.2. Hybridization and Dynamic Modelling

1. PV-CSP

Hybridization of PV with CSP is based on the prioritization of PV whenever available due to the absence of dispatchability for PV technology, while the CSP production variates to accommodate the PV production, in order to always maintain firm power output referenced to the Rankine cycle capacity of the CSP. Further details about the hybridization of PV-CSP, dispatch strategy and control system are available in [1], [69], [3].

2. PV-CCGT

In this section the hybridization of the PV and CCGT will be explained. The hybridization is done on the dynamic layer of the plant (PV-CCGT), where the PV plant output is precalculated in Matlab for each time step and an input file (PV-CCGT load file) is written and prepared before the simulation of the plant dynamic performance is started. As shown in the flow chart in figure 19, the PV-CCGT load file specifies the GT set point (E_{nom}), which is the capacity required by the GT at this time step, this value is calculated as the nominal output of the GT after subtracting the PV plant output at this specific time step. The GT net specific power output (e_{net}) is calculated as the difference between the turbine and compressor specific power output (e_t) and consumption (e_c), respectively. Using the net specific output power and the desired GT output at the specific time step, the desired mass flow rate could be calculated. This desired mass flow rate is fed to the compressor in order to obtain the desired GT output providing the total plant output when combined with the PV output. The calculated desired mass flow rate should lie in the range between M_{min} and M_{max}, which defines the minimum and maximum openings of the compressor guide vanes, this to assure that stall is avoided and max inlet air is not exceeded.

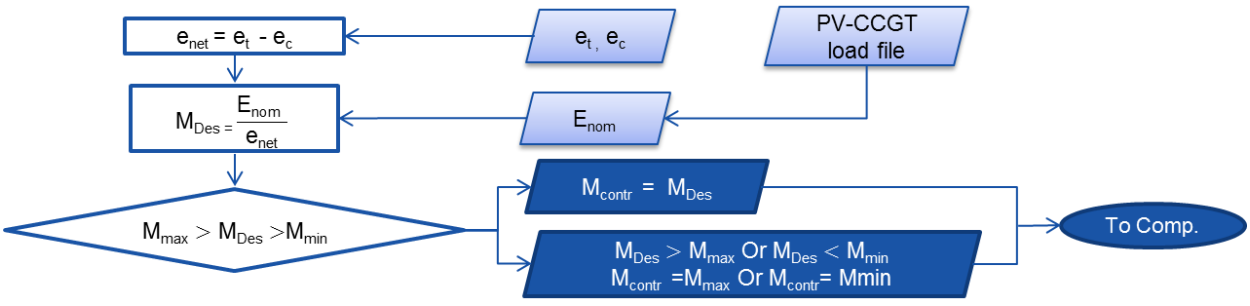

Figure 19. Hybridization of PV with CCGT flow chart

5.3. Techno-economic performance indicators

In order to evaluate the power plants under study, key performance indicators representing the technical and economic performance of the plant will be explained in details in this section.

Capacity factor (CF)

The capacity factor is calculated as shown in equation (2), by dividing the plant electricity production, represented by the summation of plant power output at each time step "$\mathrm{P_{plant,t}}$ " (1 hour is considered) along the year, over the plant nominal capacity "$\mathrm{P_{plant\ nom}}$" multiplied by number of hours in a year. This term indicates how good is the utilization of the plant referenced to a plant operating every hour in the year at rated capacity. In case of considering a hybrid plant, PV-CSP or PV-CCGT plant, $\mathrm{P_{plant,t}}$ is calculated as shown in equations (3), and (4), respectively. While $\mathrm{P_{plant\ nom}}$ is considered as the desired capacity of the plant calculated for each of the plants as shown in equations (5), and (6).

$$CF = \frac{\sum_{t=1}^{8760} P_{plant,t}}{P_{plant\ nom} * 8760} \quad (2)$$

$$P_{PV-CSP,t} = P_{CSP,t} + P_{PV,t} \quad (3)$$

$$P_{PV-CCGT,t} = P_{CCGT,t} + P_{PV,t} \quad (4)$$

$$P_{PV-CSP\ nom} = P_{CSP\ nom} \quad (5)$$

$$P_{PV-CCGT\ nom} = P_{CCGT\ nom} \quad (6)$$

Solar Share (SS)

In this study, this term is used only with the PV-CCGT plant, representing the contribution of the PV in electricity production ($P_{PV,t}$) with respect to the total plant production ($E_{PV-CCGT}$) and it is calculated as shown in equation (7), while the plant total electricity production is shown in equation (8).

$$SS = \frac{\sum_{t=1}^{8760} P_{PV,t}}{E_{PV-CCGT}} \quad (7)$$

$$E_{PV-CCGT} = E_{CCGT} + \sum_{t=1}^{8760} P_{PV,t} \quad (8)$$

Levelized cost of Electricity (LCOE)

The levelized cost of electricity is the main parameter assessing the economic performance of each technology in this study. LCOE simply gives the electricity production cost of a certain technology, so it is originally the cost of unit energy produced, normalized over the plant lifetime.

As shown in equation (9), the approach adopted in calculating LCOE in this study is based on the work of [75] and it is represented as the net present value of all costs along the plant lifetime, divided by that of the electricity produced over the plant lifetime. It is worth mentioning that the discounting of the energy term is not an indication of any physical performance of the system, but it is due to the algebraic solution of the equation[76]. The associated costs along a plant lifetime considered in this calculation are: the total capital investment (TCI), capital insurance cost ($CAPEX * k_{ins}$), decommissioning cost (C_{dec}) and operational cost ($OPEX_t$); while the total electricity production in each year is (E_t). In order to get the NPV, cash flows should be discounted, where weighted average cost of capital (WACC) was used as a discount rate, considering the cost of debt and equity and their share in the CapEx.

$$LCOE = \frac{CAPEX*k_{ins}+TCI+\sum_{t=n}^{n+n_{dec}}\frac{C_{dec}}{(1+WACC)^t}+\sum_{t=1}^{n}\frac{OPEX_t}{(1+WACC)^t}}{\sum_{t=1}^{n}\frac{E_t}{(1+WACC)^t}} = \frac{NPV(Lifetime\ Cost)}{NPV(Energy\ Output)} \quad (9)$$

Equation (10) shows the calculation of WACC where ($Eq_{\%}$) is the equity share of CapEx ($D_{\%}$) is the debt share of CapEx, (i_{eq}) is the cost of equity, (i_d) is the cost of debt, and ($Tax_{corp.}$) is the corporate tax as the interest on debt is considered after tax (tax deductible)

$$WACC = Eq_{\%} * i_{eq} + D_{\%} * i_d * \left(1 - Tax_{corp.}\right) \quad (10)$$

Total capital investment (TCI), represents the real “up-front” capital requirement considering a special interest rate during construction phase, calculation details are found in [75].

The CapEx and OpEx terms are identified for each technology in the following section, where in case of hybridization these values are added to form the total CapEx or OpEx of the hybrid plant. Cost structure for each technology will be explained in this section.

CSP plant cost structure

The cost structure of the CSP plant is divided into CapEx and OpEx, the CapEx is as shown in equation (11) accounts for the direct and indirect costs. The direct costs ($C_{CSP-direct}$) accounts for the costs of: tower (C_{Tower}), receiver cost (C_{Rec}), solar field (Heliostats) (C_{SF}), power block (C_{PB}), thermal energy storage (C_{TES}), balance of plant (including all auxiliaries)

(C_{BOP}), site cost, including site preparation, civil work and evaporation ponds (C_{Site}), and finally contingency (C_{cont}), s shown in equation (12). While the indirect cost comprises the costs of, engineering, procurement and construction (C_{EPC}), land (C_{Land}) and finally the sales tax ($C_{SalesTax}$), as shown in equation (13).

$$CAPEX_{CSP} = C_{CSP-direct} + C_{CSP-Indirect} \quad (11)$$

$$C_{CSP-direct} = C_{Tower} + C_{Rec} + C_{SF} + C_{PB} + C_{TES} + C_{BOP} + C_{Site} + C_{cont} \quad (12)$$

$$C_{CSP-Indirect} = C_{EPC} + C_{Land} + C_{SalesTax} \quad (13)$$

Regarding the CSP OpEx costs, as shown in equation (14), it consists of costs of: labor operating the plant (C_{Labor}), contractual services costs ($C_{Services}$), Utilities which represents electricity for auxiliaries, water and fuel ($C_{Utilities}$), miscellaneous costs accounting for operation overheads ($C_{Misc.}$), and finally insurance costs ($C_{ins.}$).

$$OPEX_{CSP} = C_{Labor} + C_{Services} + C_{Utilities} + C_{Misc.} + C_{ins.} \quad (14)$$

Values of all the above mentioned costs were scaled on reference plants data extracted from [18] and [40].

PV plant cost structure

The cost structure of PV plant is as well divided into CapEx and OpEx. As shown in equation (15), the PV plant CapEx is comprised of direct and indirect costs. The direct costs are represented in the cost of the PV modules ($C_{PV\ mod.}$), Inverters (C_{Inv}), tracking system and structure (C_{Track}), Balance of system including cabling electrical connections and all other auxiliaries (C_{BOS}), and contingency costs (C_{cont}) as shown in equation (16). While the indirect costs comprises of the developer costs such as overheads, developer's contingency, and other related costs excluding land (C_{Dev}), engineering and design, procurement, construction management and EPC profit (C_{EPC}), land cost (C_{Land}), and finally sales tax ($C_{SalesTax}$), as shown in equation (17).

$$CAPEX_{PV} = C_{PV-direct} + C_{PV-Indirect} \quad (15)$$

$$C_{PV-direct} = C_{PV\ mod.} + C_{Inv} + C_{Track} + C_{BOS} + C_{cont} \quad (16)$$

$$C_{PV-Indirect} = C_{Dev} + C_{EPC} + C_{Land} + C_{SalesTax} \quad (17)$$

The PV plant OpEx cost structure was much simple compared to the CSP plant, as shown in equation (18) the OpEx consists of basically two sections were the operations and maintenance contractual services ($C_{O\&M}$) is one, and the insurance costs is the other ($C_{ins.}$).

$$OPEX_{PV} = C_{O\&M} + C_{ins.} \quad (18)$$

The PV plant costs were extracted from sources [77] and [78], figures from [78] were adjusted using correlations deduced from [18] to accommodate to location of study.

CCGT plant cost structure

A new cost structure was developed for the CCGT plant in this work. The cost structure is divided into CapEx and OpEx. The CapEx is basically extracted from [79] for a complete CCGT plant, through a capacity – cost correlation. The prices are in US dollars, incoterm considered is FOB (Free on Board) factory, so shipping, insurance and custom clearance are not included according to the rules from the Incoterms® 2010 edition. The prices quoted include EPC (Engineering, Procurement and Construction) turnkey scope, including major equipment supply, plant engineering and construction.

The CCGT plant accounted for, in this extracted cost is bare bones, NG (natural gas)-fired plant, with a basic conservative steam cycle and a basic HRSG without duct firing which is generally what was developed in the model. In order to make sure that the economic model matches the technical model further cost additions were considered, such as: utilization of air-cooled condenser instead of water cooled, which accounted for an extra 10% according to [79], water treatment and waste water systems costs accounted for an added 4% considering power block costs from [18]. Developer cost was extracted from [80] after comparisons with figures from [81] and [18]. Contingency cost was determined through considering figures from [82], [18], and [83].

CapEx structure of CCGT plant could be summarized in equation (19), where the CCGT CapEx ($CAPEX_{CCGT}$) comprises of: total cost of plant ($C_{plant\ total}$) and indirect costs ($C_{indirect}$). The total cost of plant, as shown in equation (20), considers (C_{plant}) representing the plant cost considering air-cooled condenser and including EPC, the water treatment and waste water systems cost ($C_{water\ treat.}$), and developer cost ($C_{Dev.}$). Finally, indirect cost is basically the contingency cost (C_{cont}) and sales tax ($C_{Sales\ Tax}$) as shown in equation (21).

$$CAPEX_{CCGT} = C_{plant\ total} + C_{indirect} \quad (19)$$

$$C_{plant\ total} = C_{plant} + C_{water\ treat.} + C_{Dev.} \quad (20)$$

$$C_{indirect} = C_{cont} + C_{Sales\ Tax} \quad (21)$$

The OpEx structure of CCGT plant is divided into maintenance and operation costs as shown in equation (22). Maintenance costs comprises of fixed and variable costs as shown in equation (23), where the fixed costs are always associated with the plant capacity and is independent on hours of operation or electricity production, on the other hand the variable

costs are depending on the plant operation and electricity production. Operation costs comprises of fuel and water cost as shown in equation (24).

$$OPEX_{CCGT} = C_{maint} + C_{oper} \quad (22)$$

$$C_{maint} = C_{fixed} + C_{variable} \quad (23)$$

$$C_{Oper} = C_{fuel} + C_{water} \quad (24)$$

Fixed and variable operation and maintenance costs were deduced based on extractions from [80], [81], [84], [85], and developed correlations between certain costs at different location based on data from [18]. Fuel (natural gas) and water costs were extracted from [86] for this location of study.

6. Multi Objective Optimization

Techno-economic analysis of power plants considers many conflicting objectives, as plants for example, might be required to produce maximum possible electricity (achieve high capacity factor), yet, at minimum costs, or if it is a hybrid plant involving fossil fuels, it might be required to have maximum renewable contribution yet, with minimum capital investments. There are several examples for such cases, but the common thing is that those objectives are conflicting in the majority of the cases. Accordingly, no single optimum could be obtained for all objectives, and for examining the trade-offs between different objectives, multi-objective optimization (MOO) comes in handy.

Using such optimizer provides the possibility of examining different trade-offs and helps decision makers to select the desired compromise between the objectives of concern. DYESOPT comprises a modified version of Queuing Multi-Objective Optimizer (QMOO)[9], [87], an evolutionary algorithm, which is a part of a wider class of routines known as population-based algorithms, which works in a way that it maintains a population of designs, set by resolution of the model, this population is moved towards a group of optimal designs through evolution[74]. This process ends with a development of a Pareto-optimal front, which is an optimal trade-off curve formed by several Pareto-optimal designs. These are designs which no other design exists that is simultaneously better in all objectives [87].

An example of Pareto optimal front is shown in figure 20, where the 2 objectives are favored at the two extreme, each on the expense of the other, and moving away from the Pareto front towards any other solution in the feasible region makes one objective worse, providing a “naïve” solution. [74]

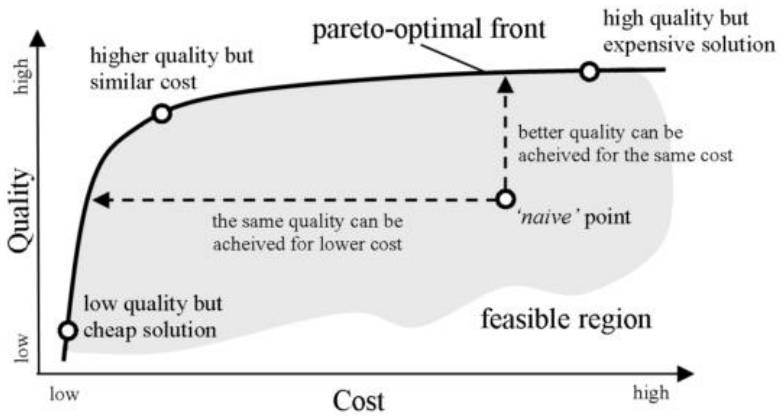

Figure 20. General example of a Pareto-optimal front [74]

This optimizer has been developed at the Industrial Energy Systems Laboratory of the Swiss Federal Institute of Technology in Lausanne. [9], [74]

6.1. Optimization Cases

The location selected for this study is designated 24.3 N and 55.6 E, which is about 50 Km South the flagship project “Sheikh Mohammad Bin Rashid Al-Maktoum Solar Park”. At this location, the weather data used was a Typical Meteorological Year (TMY) extracted from Meteonorm, a weather database which is considered the meteorological reference for solar energy and other applications.

After the PV-CCGT model was implemented, the CSP and CSP-PV models were accommodated to the study case - in terms of weather data, cost functions, technical and economic input parameters -, cases were identified for running multi-objective optimizations, while variating critical design parameters, to obtain the optimum configuration of each technology based on two conflicting objectives.

These objectives are maximizing the capacity factor (CF) which is an important technical KPI, and minimizing the levelized cost of electricity (LCOE) which is the most important economic KPI in the case under study. The two objectives are clearly conflicting in the case of CSP and PV-CSP power plants, where in order to obtain a higher capacity factor, a higher solar multiple (SM) is required, which leads to an increase in the size of the solar field. Larger storage facility is needed as well. Both are needed in order to cover the required capacity for a longer period. Consequently the plant CapEx increases significantly, which directly increase the LCOE. In PV-CSP, the impact of raising the CF is expected to be less than the CSP case, due to the fact that the PV contribution is basically a cheaper alternative instead of enlarging the solar field.

The PV-CCGT case is different, as the desired capacity factor will be reached anyway through supplying more natural gas to the combined cycle to accommodate for the remaining capacity unmet by the PV part. The desired objectives in this case are maximizing the solar share and minimizing the LCOE, which are as well conflicting, as increasing the solar share means enlarging the solar part of the plant which is the more CapEx intensive and accordingly leads to a higher LCOE.

The evaluation of each MOO for each technology will be thoroughly discussed and the optimum configurations obtained for each case will be evaluated against each other to provide a profound comparison of the 3 different power plant configurations/technologies for the selected location. As shown in table 2 and 3, two cases were identified for each power plant configuration (CSP, PV-CSP, and PV-CCGT) based on the dispatch strategy.

The first case was for designing the plant for baseload operation, while variating the power plant capacity, in order to observe the power plant configurations at which the models tends to converge. As well as, how critical design parameters variate to achieve the two conflicting objectives, the trade-off between the two conflicting objectives, and the optimum capacity for each technology considering the 2 selected objectives. The design variables applied in the first case are mentioned below in table 2, with the ranges used for each variable for each technology.

Design Variable	CSP	PV-CSP	PV-CCGT	Unit
Solar multiple	[1, 4]	[1, 4]	-	[-]
Tower height	[180, 280]	[180, 280]	-	[m]
Storage size	[1, 24]	[1, 24]	-	[h]
CSP net power	[50, 350]	[50, 350]	-	[MWe]
PV net power	-	[0, 450]	[10, 400]	[MWe]
Array – Inverter ratio	-	[1, 2]	[1, 2]	[-]
GT Nominal Capacity	-	-	[100, 400]	[MW]
Min. GT load	-	-	[0.1, 1]	[-]
Evaluations	2330	2261	2334	[#]

Table 2. Design variables for optimizations of baseload cases

The second case was for designing the plant for firm power output operation from 6:00 to 21:00 following the typical daily load profile mentioned earlier. In this case, a fixed capacity for the power plant is set to 200 MW, as it is the capacity announced for the first CSP project in the flagship solar park in Dubai [48]. The objective of running this case is to identify the optimum configuration with the formerly specified capacity and with variating the selected critical design parameters, for each power plant and be able to have a consistent comparison between the three technologies under study. The design variables applied in the second case are mentioned below in table 3, with the ranges used for each variable for each technology.

Design Variable	CSP	PV-CSP	PV-CCGT	Unit
Solar multiple	[1, 4]	[1, 4]	-	[-]
Tower height	[180, 280]	[180, 280]	-	[m]
Storage size	[1, 24]	[1, 24]	-	[h]
PV net power	-	[0, 450]	[10, 400]	[MWe]
Array – Inverter ratio	-	[1, 2]	[1, 2]	[-]
Min. GT load	-	-	[0.1, 1]	[-]
Evaluations	2334	2334	2334	[#]

Table 3. Design variables for optimizations of firm power 6:00 to 21:00 cases

6.2. Results and discussion

As mentioned formerly, two cases are studied for each of the three technologies (CSP, PV-CSP and PVCCGT), accordingly six optimizations were performed. Three of which are considering baseload dispatch with variable plant capacity, the other three considers firm power output of 200 MW for 15 hours, 6:00 to 21:00. In this section, the results of those six optimizations will be presented, with an explanation for each case elaborating the trade-off between the selected objectives, the optimum plant selection, and the effect of varying the critical design parameters on the trade-offs. Each of the plots presented in this section is a result of more than 2000 evaluations which are represented as dots on the plots, each of which represents a specific plant configuration with a combination of the design variables mentioned in table 2 or 3. The optimum plants are the set of dots forming the Pareto front with each extreme favoring one of the objectives and the trade-off is at the curve bent; while the dots confined by this front are considered as naive solutions.

6.2.1. CSP

6.2.1.1. CSP baseload:

In the following plots, the results of the optimizations run for CSP technology in baseload operation with variable capacities are shown. Objectives targeted are Maximum capacity factor and minimum LCOE, through variating some key parameters, shown in table 2. Different key parameters are shown as a third variable on the plots to compare their relation with the optimization results. The baseload optimizations were performed without fixing the capacities, in order to show the favored plant capacity according to the case-study. The results show a Pareto front with optimum plants ranging from 50% to 80% in CF, while LCOE values in a range from 145 to 180 USD/MWh. The relation of plant capacity with the 2 mentioned objectives is shown in figure 21. The optimization converged to a range of plant capacities of 50 to about 175 MW. The trade-off region is clearly favoring a 100-130 MW plant capacity.

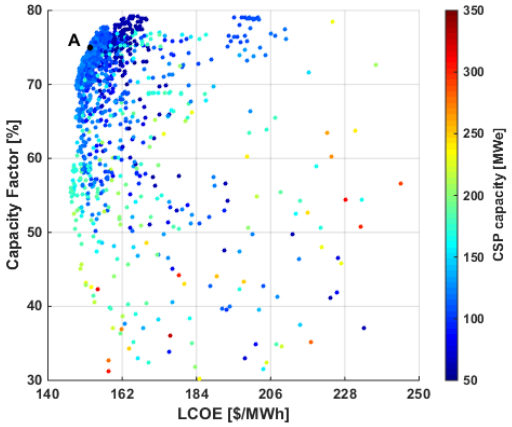

Figure 21. CSP results in baseload operation – CSP capacity

The relation of SM and TES size with the selected objectives are shown in figures 22 (a) and (b), respectively. High SM values and TES sizes will be needed in order to achieve high capacity factors which is clearly shown in figures 22 (a) and (b), this directly impacts the LCOE, but through optimizations plant capacity was compromised to achieve both high CF and low LCOE, resulting in optimum plants for highest CFs are of low capacities about 50 MW as shown in figure 21.

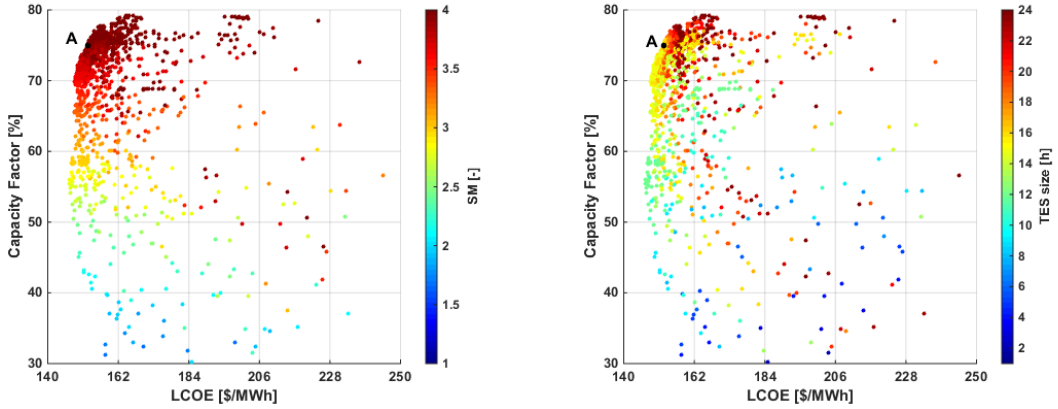

(a) (b)

Figure 22. CSP results in baseload operation: (a) SM (b) TES size

The last plot for the results of this case is shown below representing the CapEx in figure 23. The CapEx of plants with solar multiple mentioned in the previous paragraph are shown as of a low range (light blue color), although these plants have a high SM and TES size, yet are of low capacities (around 50 MW) resulting in a relatively lower CapEx. While plants of the trade-off region where optimum plant “A” was selected are shown in orange to red color range, reflecting higher CapEx due to their larger capacities (100 to 130 MW).

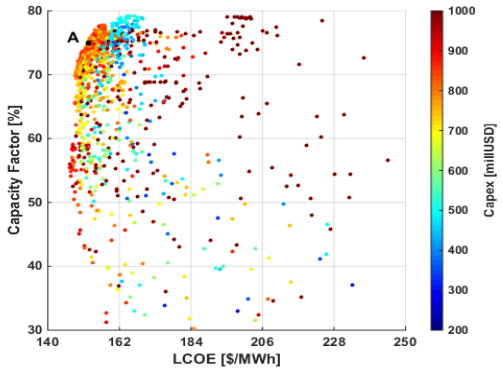

Figure 23. CSP results in baseload operation: CapEx

Optimum plant “A” was selected for CSP technology in baseload operation. The choice was based on 2 criteria, the first is a 75% CF. This CF was chosen as it is the highest reasonable CF that could be achieved within this optimization, providing a fair trade-off between both selected objectives, almost center of the trade-off region. Minimum LCOE was the second criterion for identifying the plant. Plant “A” key parameters and performance indicators are mentioned in table 4. Further discussion will be presented in the “CSP optimum plants dynamic performance” section.

6.2.1.2. CSP firm power 6-21

The following plots show the results of CSP technology in firm power output operation from 6:00 to 21:00 for a fixed plant capacity of 200 MW. The results plots elaborate the optimum plants designed in order to achieve minimum LCOE and maximum CF, through variating some key parameters, shown in table 3. The plots involve a third key parameter to be observed VS the two conflicting objectives. The results shows a clear Pareto front of CF ranging from 43% till 56% and LCOE ranging from around 160 to 250 USD/MWh. Higher capacity factors require higher SM and TES size as shown in figures 24 (a) and (b) respectively. As operating for more hours supplying firm output, requires a higher SM and larger storage capacities in order to generate during hours with low irradiance or night hours.

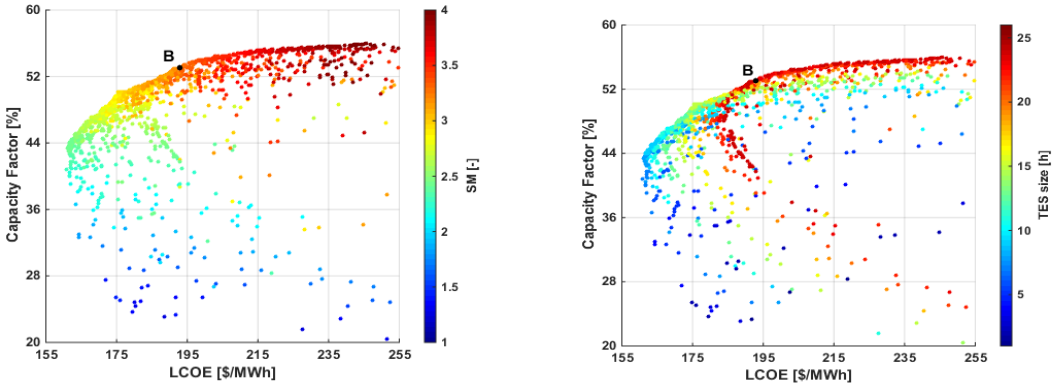

(a) (b)

Figure 24. CSP results in firm power 6:00 to 21:00 operation: (a) SM (b) TES size

Eventually, by increasing SM and TES size for higher capacity factor, the plant CapEx increases, which is clearly shown in figure 25, where the variation between low CF of 44% to high (relatively) 55% reflects an increase of more than 85% of the CapEx. As clearly shown as well, the CapEx increment per unit increase in CF, at high CF ranges is much higher than that in low CF ranges.

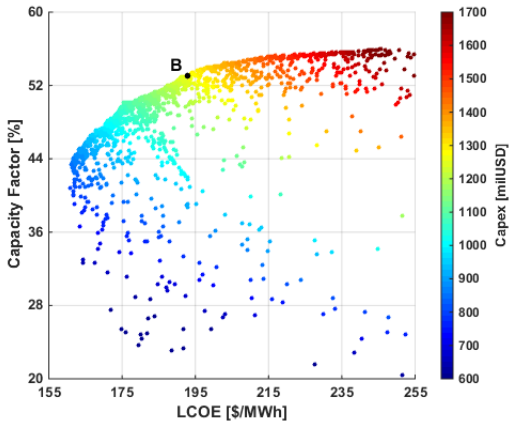

Figure 25. CSP results in firm power 6:00 to 21:00 operation: CapEx

Optimum plant “B” was selected from the Pareto front of this optimization case. The selection was based on a CF of 53.1, representing 85% of the theoretical maximum CF of the case under study. The specific 85% choice, will be explained in the selection of the optimum plant of PVCCGT 6:00 to 21:00 case. Minimum LCOE was the second criterion identifying the optimum plant for this case. Plant B lies in the trade-off region compromising both objectives (minimum LCOE and maximum CF). Plant “B” key parameters and performance indicators are mentioned in table 4. Further discussion will be presented in the following section (CSP optimum plants dynamic performance).

6.2.1.3. CSP optimum plants dynamic performance

In this section the two CSP optimum plants selected for each dispatch strategy will be discussed in deeper details through the key parameters and the dynamic performance through a plot of a 1 week operation. This section does not provide a comparison between the mentioned plants, as each provide a different dispatch strategy. The week selected shows a significant variation of solar resource, and accordingly provides a clear performance of the model at its extremes. This week will be fixed in all further dynamic performance plots for the sake of comparative analysis in following sections. Table 4 shows the key design parameters of the plants under study in both dispatch strategies. As mentioned earlier these plants are not the absolute optimum plants for this technology in this case study, but these are of the optimum plants selected from the Pareto front of the optimizations performed.

Variable	*A*	*B*	*Unit*
Plant type	CSP	CSP	[-]
CSP capacity	113	200	[MW]
TES size	16	24	[h]
Solar multiple	3.93	3.23	[-]
Number of Heliostats	21804	32290	[#]
Dispatch strategy	Baseload	6:00-21:00	[-]
Tower height	266	280	[m]
KPIs and key figures	***A***	***B***	***Unit***
CF	75	53.1	[%]
LCOE	152.47	192.78	[USD/MWhe]
CapEx	798.7	1268.1	[milUSD]
OpEx	12.5	19.5	[milUSD/Year]
Electricity production	742.79	930.36	[GWhe/Year]
Specific cost	7063	6341	[USD/KWe]

Table 4. CSP optimum plants parameters and key figures

Figure 26 shows the dynamic performance of plant A, a CSP plant in baseload operation. The plant is a CSP-only plant of 113 MW capacity and a 16 hours storage facility (TES), the plant is equipped with a solar field comprising of 21804 Heliostats with a single tower 266 m high, resulting in a SM of 3.9. The 1 year performance simulation resulted in a CF of 75%, with an electricity production of about 743 GWhe.

The dynamic performance shows the perfect operation of the plant (CSP power plotted in blue) in the first day, due to the availability of good DNI reflected in the field power plot colored in yellow and the partially charged TES. As shown the TES level (plotted with the black dotted line) drops during the discharge at night (when the field power is not available), then the plant shuts down due to the empty storage and irradiation unavailability. On the next day (Monday), the available DNI is sufficient to partially charge the TES and operate the plant for only few hours during the night. Due to bad DNI and empty TES, the plant remains in shutdown for 2 consecutive days. In the 5^{th} day the plant operate for only few hours for same reasons, and finally the 2 remaining days provides an example of how the plant should be working in normal conditions. A good DNI is available to fully charge the TES, and operate the plant during the day, then the fully charged TES, keeps the plant running during the night till the next day, which comes in average DNI that partially recharges the TES and full load operation is sustained for 2 consecutive days. Finally, the thermo-economic calculations resulted in a total plant CapEx of about 800 milUSD, OpEx of 12.5 milUSD and an LCOE of 152.5 USD/MWhe.

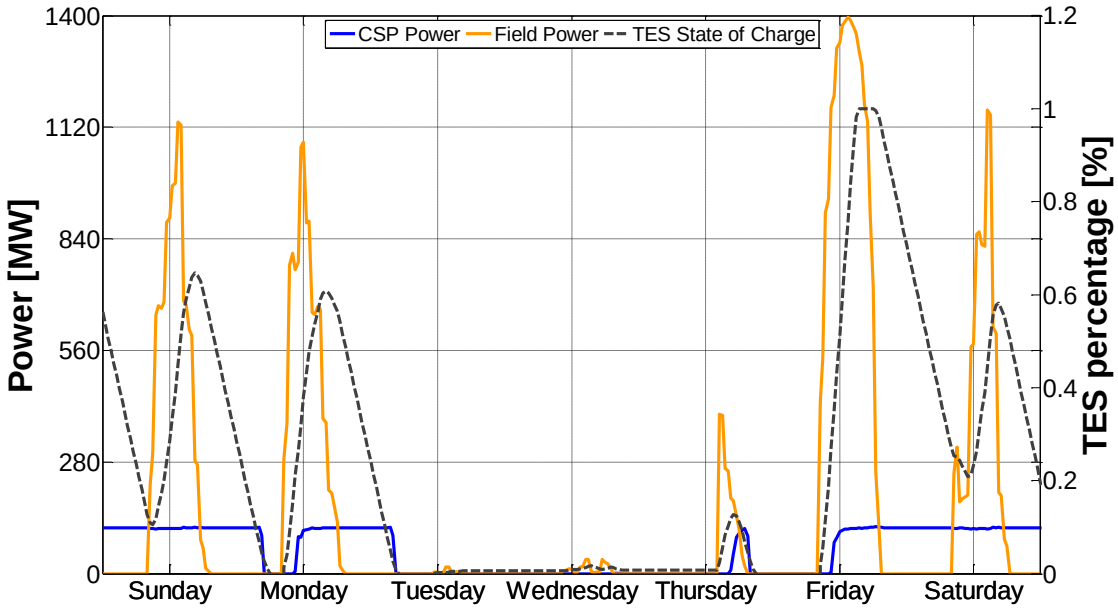

Figure 26. Plant A - CSP baseload operation winter week

Figure 27 shows the dynamic performance of plant B, a CSP plant in 6:00 to 21:00 of firm power operation. The plant is a pure CSP plant of 200 MW capacity, which will be fixed in all other optimum plants in firm power operation (6:00 to 21:00) for further comparative analysis. The plant includes a 24 hour storage facility (TES), and equipped with a solar field comprising of 32290 Heliostats with a single tower 280 m high, resulting in a SM of 3.23. The 1 year performance simulation resulted in a CF of 53.1 %, with an electricity production of about 930 GWhe.

The same week of baseload operation was chosen for showing the performance in the firm power operation, which is quite similar to that of baseload, except for the daily shutdown and start-up of the plant. The week starts with the same 2 days with good DNI, but in this case the 6:00 to 21:00 firm power was achieved without interruptions, extended to the third day despite of poor DNI, mitigated by the SM and the storage capacity. The 4th and the 5th day operation was interrupted due to empty storage and very poor DNI, and then restored again with improving DNI.

Finally, the thermo-economic calculations after simulating 1 year of operation, resulted in a total plant CapEx of about 1268 milUSD, OpEx of 19.5 milUSD and an LCOE of 193 USD/MWhe.

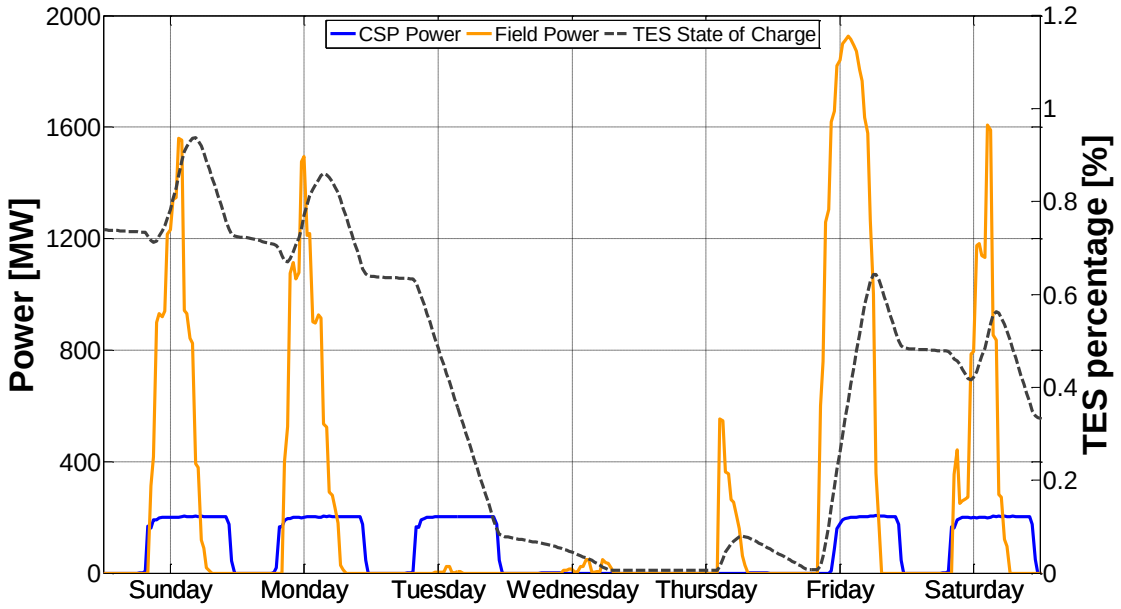

Figure 27. Plant B - CSP 6:00 to 21:00 winter week

6.2.2. PV-CSP

6.2.2.1. PV-CSP baseload: "C" & "C*"

The plots in this section show the result of optimization of PV-CSP technology in baseload operation without fixing the plant capacity. The objectives set for this optimization were the same as that in the CSP, maximum capacity factor and minimum LCOE, while variating some key parameters, shown in table 2. The results show a clear Pareto front of optimum plants covering a CF ranging from 65% up to almost 93%, versus LCOE ranging from about 150 to about 290 USD/MWh. The optimization converged to plants with CSP plant capacities in the range of 100 to 170 MW, which could be seen clearly in the trade-off region in figure 28 (a), while smaller plants were favored for a slight increase in capacity factor, but those small plants are complemented with a larger PV plant capacity reaching to 4 times as big as the CSP as shown in figure 28 (b). Capacity ratio PV/CSP goes back from 4 to an optimum of 0.75 to 1 in the trade-off region.

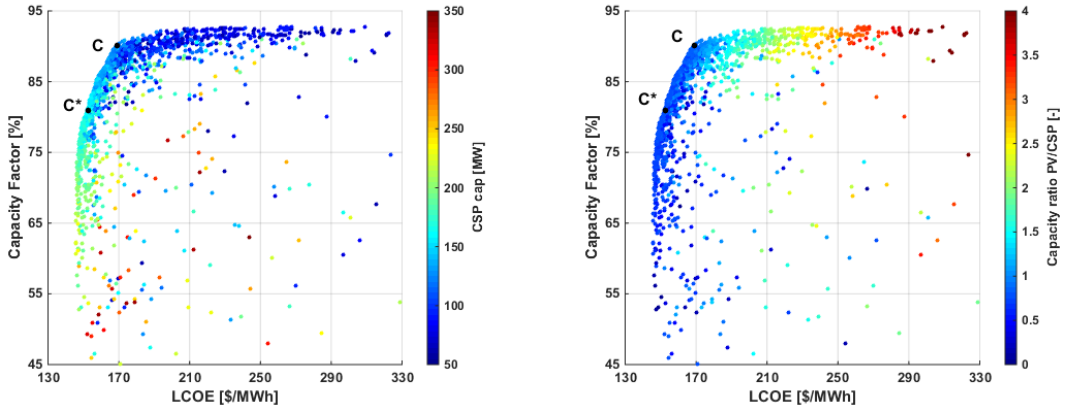

(a) (b)

Figure 28. PV-CSP results in baseload operation: (a) CSP cap (b) Capacity ratio PV/CSP

Figure 29 (a) and (b), clearly explain how such high capacity factor is reached from a solar based technology. Larger solar field coupled with large storage capacities provide dispatchability to this technology, accordingly in both figures, CF higher than 85% are dominated with orange to red color, elaborating a SM range from 3 to 4 and a storage capacity ranging from 16 to 24. This could be easily explained as higher SM are needed in order to provide excess energy for charging a larger storage that would allow the operation of the plant during the night or hours with weak DNI.

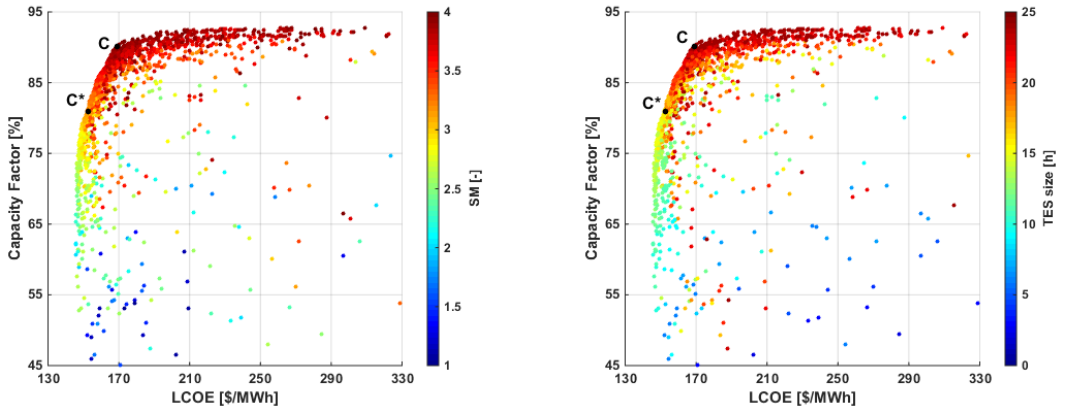

(a) (b)

Figure 29. PV-CSP results in baseload operation: (a) SM (b) TES size

The relation of CapEx with the two conflicting objectives chosen is shown in figure 30, where the variation across the whole Pareto front, only ranges from 900 to 1300 milUSD. The CSP plant capacity and solar multiple are 2 parameters that have a significant impact on the total plant CapEx. A certain balance is sustained in this optimization that resulted in this small variation in CapEx, larger capacities were chosen with low CF, the higher the CF the smaller the CSP capacity gets, till the trade-off and then higher contribution of PV is provided with

smaller CSP capacities, which results in lower CapEx as PV replaces a significant part from the SF for less cost.

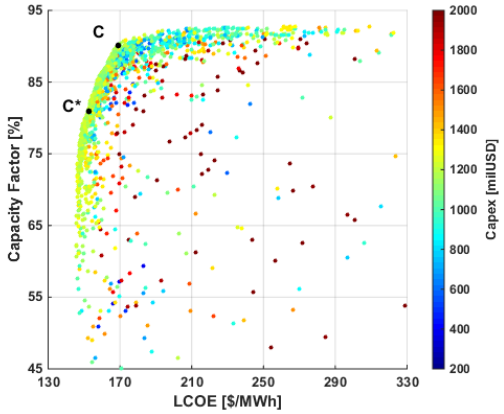

Figure 30. . PV-CSP results in baseload operation: CapEx

The optimum plant chosen in this case was plant “C”, which was easily chosen at an estimated trade-off point clearly distinguishable in this optimization, providing a perfect compromise between maximum CF and minimum LCOE. Another optimum plant “C*”, was selected in this case, for the sake of comparison with the corresponding CSP optimization, where the exact LCOE value achieved by the plant is used in this optimization result to choose the maximum CF achieved at this LCOE, proving the case that hybridization with PV provides higher CF for the same LCOE, or in other words: “contributes in lowering the overall plant LCOE”. Plants “C” and “C*” key parameters and performance indicators are mentioned in table 5. Further discussion will be presented in the (PV-CSP optimum plants dynamic performance) section.

6.2.2.2. PV-CSP firm power 6-21: “D”

In this section, the results obtained from the optimization run of PV-CSP model in firm power production dispatch strategy, with a CSP capacity of 200 MW, while variating some key parameters shown in table 3. The results show a clear Pareto front, quite similar to that of the baseload. CF ranges from about 42% to about 58%, versus LCOE range of around 160 to 300 USD/MWh. Figure 31 (a) shows the CapEx values of the plotted pants, in order to achieve higher CFs for a certain capacity, higher initial investments are needed, which directly impact the LCOE, specially on the top section of the Pareto front, where the investments are much higher than the benefit of the corresponding increase in CF. Figure 31 (b) shows capacity ratio of PV/CSP, where it is clear that for optimum plants, the ratio would be in the range from 0.5 to 0.9, favoring high PV contribution for high CFs.

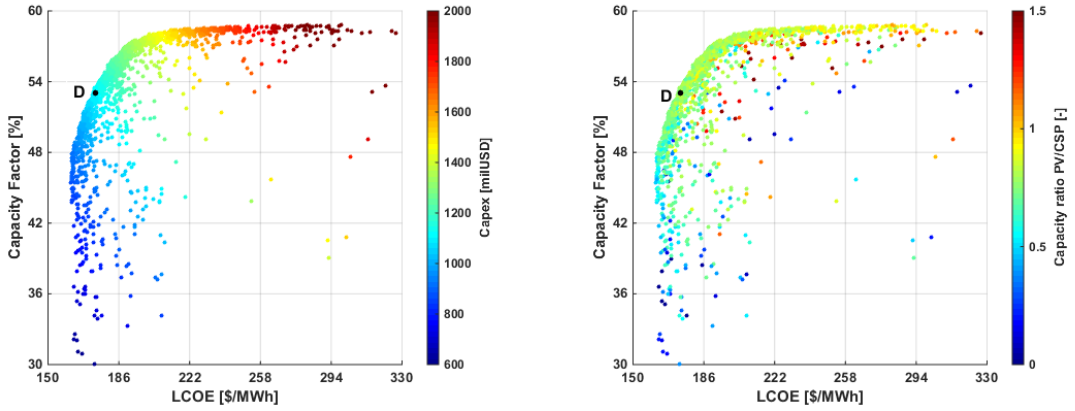

Figure 31. PV-CSP results in firm power 6:00 to 21:00 operation: (a) CapEx (b) Capacity ratio PV/CSP

The CapEx plot in figure 31 (a), could be clearly explained from the below plots in figure 32 (a) and (b). As high CF are associated with higher SM and TES size as explained in the cases of CSP, this is directly reflected on the plant CapEx as the solar field is the most CapEx intensive part of the CSP plant.

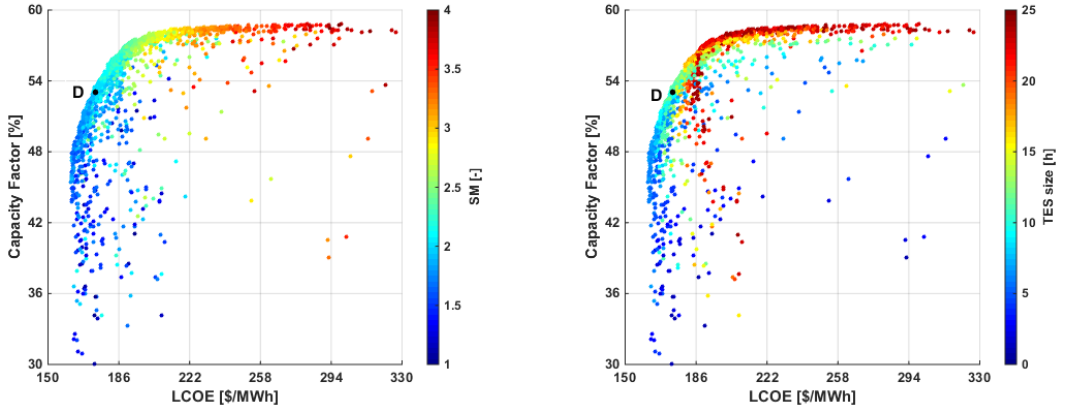

Figure 32. PV-CSP results in firm power 6:00 to 21:00 operation: (a) SM (b) TES size

The plot in figure 33 shows the curtailed PV for each of the plants involved in the CF-LCOE relation. It could be observed that plants achieving high CF, are characterized with high curtailment of PV production, which results in higher LCOE as well, due to the fact that CapEx spent on high PV capacities installed does not return in an equivalent higher electricity production.

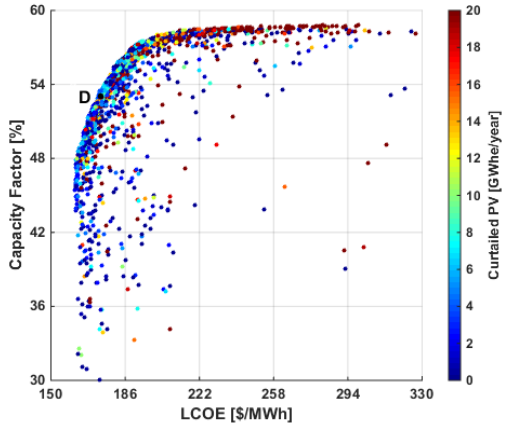

Figure 33. PV-CSP results in firm power 6:00 to 21:00 operation: Curtailed PV

Optimum plant “D” was selected from the Pareto front of this optimization case. The selection was based on a CF of 53.1, representing 85% of the theoretical maximum CF of the case under study. The specific 85% choice, will be explained in the selection of the optimum plant of PVCCGT 6:00 to 21:00 case. Minimum LCOE was the second criterion identifying the optimum plant for this case. Plant B lies in the trade-off region compromising both objectives (minimum LCOE and maximum CF). Plant “D” key parameters and performance indicators are mentioned in table 5. Further discussion will be presented in the following section (PV-CSP optimum plants dynamic performance).

6.2.2.3. PV-CSP optimum plants dynamic performance

In this section the two PV-CSP optimum plants (C & D), selected for each dispatch strategy will be discussed in deeper details through the key parameters and the dynamic performance through a plot of a 1 week operation. Plant C* is presented for sake of comparison with pure CSP plant A. This section does not provide a comparison between the mentioned plants (of the same technology), as each provide a different dispatch strategy. As mentioned in the CSP results section, the week selected is the exact same of the previous 2 cases for the sake of comparative analysis in following sections. Table 5 shows the key design parameters of the plants under study in both dispatch strategies.

Variable	*C*	*C**	*D*	*Unit*
Plant type	PV-CSP	PV-CSP	PV-CSP	[-]
CSP capacity	122	145	200	[MW]
TES size	24	16	11	[h]
Solar multiple	3.98	3.18	1.97	[-]
Tower height	279	270	261	[m]
Number of Heliostats	23698	22160	17746	[#]
PV/CSP cap. ratio	0.85	0.74	0.72	[-]
PV capacity	104	107	155	[MWac]
Tracking	Single-Axis	Single-Axis	Single-Axis	[-]
Dispatch strategy	Baseload	Baseload	6:00-21:00	[-]
KPIs and key figures	***C***	***C****	***D***	***Unit***
CF	90	80	53.1	[%]
Electricity production	965.38	1028.59	930.1	[GWhe/Year]
Curtailed PV	21.4	0.1	2.25	[GWhe/Year]
LCOE	169.07	152.41	173.9	[USD/MWhe]
CapEx	911.6	852.9	763.6	[milUSD]
OpEx	13.7	13.3	13.4	[milUSD/Year]
Plant Specific cost	9327.2	7522	5537	[USD/KWe]

Table 5. PV-CSP optimum plants parameters and key figures

Figure 34 shows the dynamic performance of plant C, a PV-CSP plant operating as baseload, of a 122 MW CSP plant associated with a TES of 24 hours and a SM of 3.98 capacity, hybridized with 104 MW(AC) of PV with single-axis tracking. The 1 year performance simulation resulted in a CF of 90%, with an electricity production of about 965 GWhe. The figure shows the performance of the hybridized plant, with the same legend used as the CSP plots, adding the Net Electrical Power and the PV in red and green, respectively.

The PV is prioritized whenever available to provide the needed production, while the CSP plant provide the rest, in addition to charging the TES for night hours production, The first 2 days operated perfectly with the TES almost fully charged at the beginning of each day, while on the third day, the DNI was quite low, that the TES provided the needed capacity through almost the whole duration, while the PV contributed with a minor capacity as shown in the plot, with the CSP creating the trough in blue, accommodating the PV crest in green to assure firm output of 122 MW. The thermo-economic calculations resulted in a total CapEx of 912 milUSD, OpEx of 13.7 milUSD, and an LCOE of 169.07 USD/MWhe.

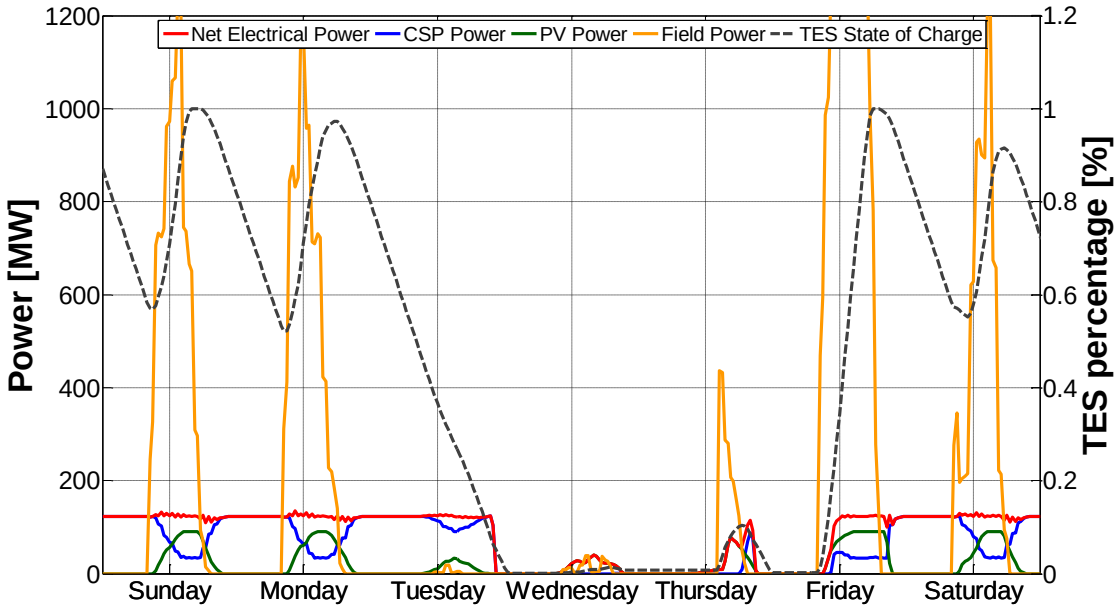

Figure 34. Plant C - PV-CSP baseload operation winter week

Figure 35 shows the dynamic performance of plant D, a PV-CSP plant operating from 6:00 to 21:00 providing firm power, of a 200 MW CSP plant associated with a TES of 11 hours and a SM of 1.97, hybridized with 155 MWac of PV with single-axis tracking. The 1 year performance simulation resulted in a CF of 53.1%, with an electricity production of about 930 GWhe. The figure shows the performance of the hybridized plant, with the same legend used in the PV-CSP baseload plot in figure 34.

The dynamic performance is very similar to that of the baseload, except for the case of operating within a window (6:00 to 21:00). It is obvious for this plant configuration, a smaller TES and SM compared to the baseload case, as less hours are need to be covered, yet still not enough for covering the load during consecutive days with bad DNI. The thermo-economic calculations resulted in a total CapEx of 764 milUSD, OpEx of 13.4 milUSD, and an LCOE of 174 USD/MWhe.

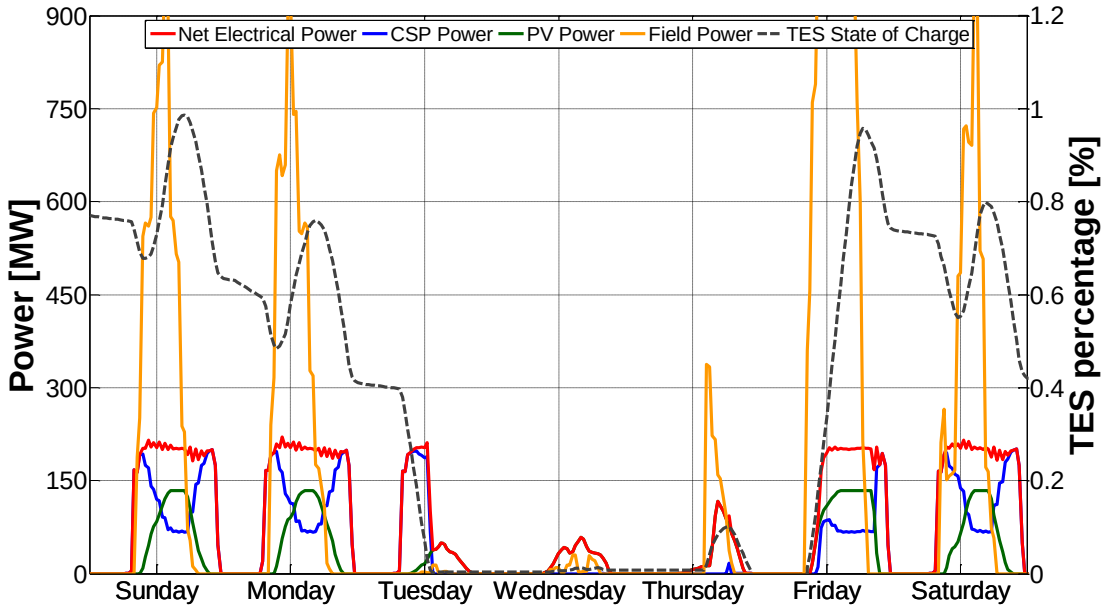

Figure 35. Plant D - PV-CSP 6:00 to 21:00 operation winter week

Plant C* was selected from the baseload optimization Pareto front with the same LCOE as plant A (CSP), in order to compare both technologies in terms of CF reached for a certain LCOE. As shown, for the LCOE of 152 USD/MWhe, CSP optimum plant reached a CF of 75%, while that of the PV-CSP reached a CF of 80%. In other words, hybridization of CSP with PV reduces the plant LCOE. This will be reassured through comparison of firm output plants of the same CSP capacity and CF, to provide a more solid evidence.

6.2.3. PV-CCGT

6.2.3.1. PV-CCGT baseload “E”

The following set of figures show the optimizations of PV-CCGT technology in baseload operation strategy. The trade-offs between maximizing solar share and minimizing LCOE, considering a critical design variable or a key figure/KPI as a third variable on the plot. The results are based on the developed model in baseload dispatch strategy, while varying the design parameters in table 2, without fixing the CCGT plant capacity. As shown in all plots (36 till 38) the model tends to converge to a well clear and defined Pareto front, with minimum solar share and minimum LCOE at one side, maximum solar share with maximum LCOE at the other, and the trade-off between minimum LCOE and maximum solar share at the top left corner, where the optimum plant was selected.

Figure 36(a) shows the CCGT capacity as a third variable on the plot. As the plant capacity was not fixed, the optimization converged to large CCGT capacities for achieving lower

LCOE as economies of scale is quite significant in CCGT technology, this is clearly observed as well from the cost correlation at which the cost structure of this technology is based in this model, formerly mentioned. On the other hand, smaller capacities of CCGT plants were used with higher solar shares and higher LCOE. Figure 36(b), shows the PV installed capacity as a ratio of the CCGT capacity as the third variable, where it is clear that for achieving higher solar shares larger PV capacities will be required which will result in higher LCOEs and more expensive power plants. As mentioned in the hybridization section the PV max. output is limited by the CCGT nominal capacity for producing firm output and the excess is curtailed. Accordingly the only way to maximize the solar share is to add much larger capacities compared to that of the CCGT (higher PV/CCGT capacity ratio) in order to reach the needed firm output earlier in the day. This will result in larger curtailed PV output, which is considered as low utilization of the plant and reflects higher LCOE. This is clearly obvious from figure 36 (c), as minimal curtailment is achieved with PV/CCGT capacity ratio (ranging from 0 to about 1), reaching solar share of about 29%, and in order to increase 4-5% more, the PV capacity should jump from 1 to 2.5 times the CCGT capacity.

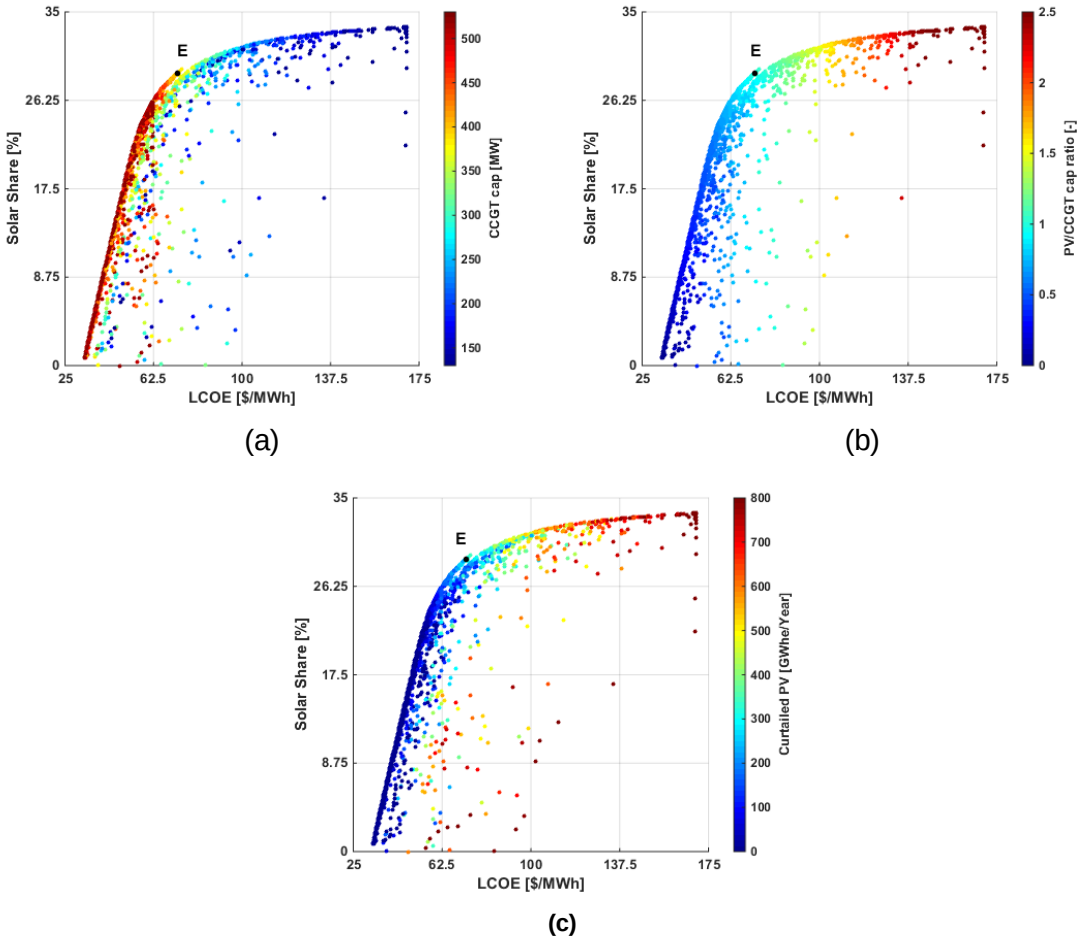

Figure 36. PV-CCGT results in baseload operation: (a) CCGT cap (b) CapEx (c) Curtailed PV

Larger PV capacities require higher investments (CapEx), as shown in figure 37 (a). The trade-off region shows the highest CapEx region, as it has medium-large (350 MW - 450 MW) sized CCGT plants and a unity PV/CCGT capacity ratio, which means large PV plants as well. As shown in figure 37(b), the plant specific cost converges to about 1000 USD/kWe when it goes to the extreme of the lowest LCOE/solar share represented by almost pure and large CCGT plant, while it converges to about 1800 USD/kWe when it goes to the other extreme of maximum solar share/LCOE, which is represented by a configuration dominated by PV. In the optimum plants section, it will be elaborated that a large size CCGT specific cost is around 1000 USD/kWe, while the PV specific cost is around 1800 USD/kWe, which perfectly matches the above configurations. These values are based on the cost structure assumed in this study.

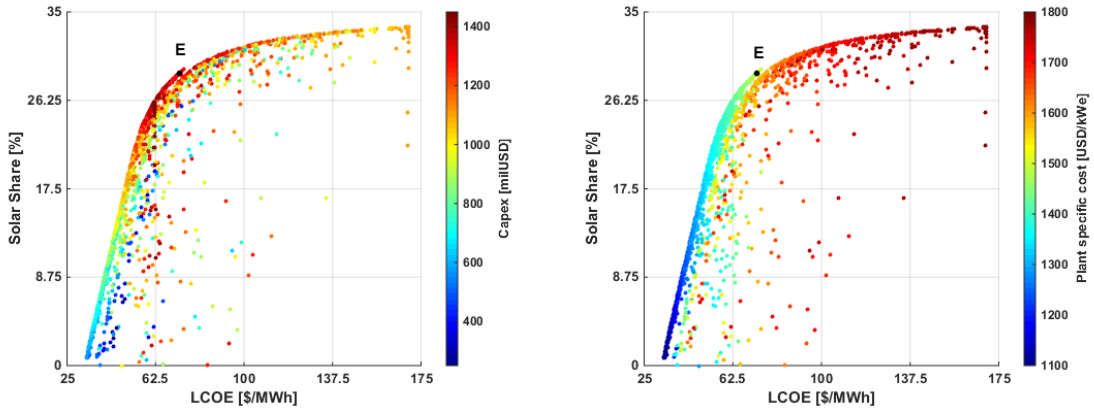

Figure 37. PV-CCGT results in baseload operation: (a) CapEx (b) Plant specific cost

The main reason behind the hybridization of CCGT with PV goes back to the reduction of natural gas consumption to reduce OpEx and carbon emissions, which is straight forward, the higher the solar share the less operational expenses and less emission as shown in 38 (a) and (b), respectively.

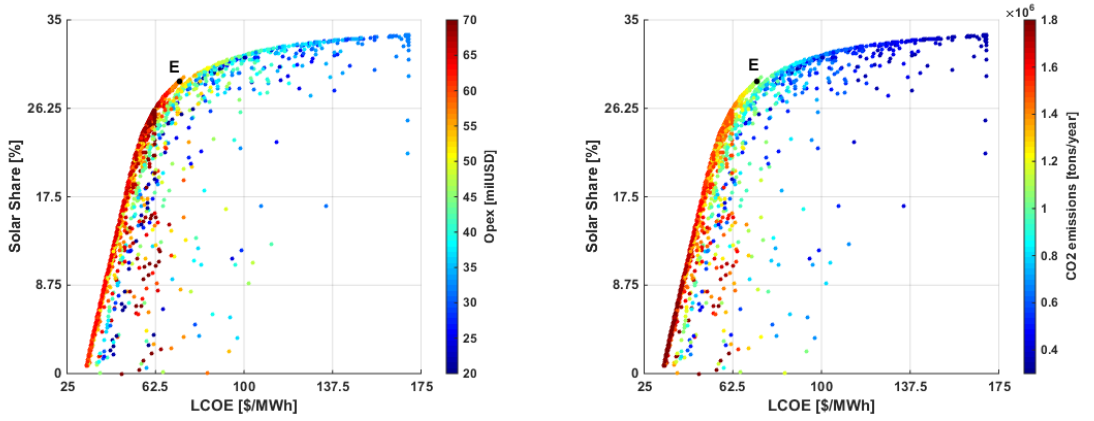

Figure 38. PV-CCGT results in baseload operation: (a) OpEx (b) CO2 emissions

The gas turbine minimum operation load factor was set as a variable, and almost all the optimum plants converged to around 10%, which is the minimum value of this parameter. This is due to the fact that the lower minimum operation load factor provides better hybridization with PV, which will result in higher utilization of PV production, less curtailment, better LCOE and higher solar share.

Plant “E” was chosen as an optimum plant for PV-CCGT technology in baseload operation. The choice was based on having a trade-off between the 2 objectives, where a solar share of about 29% centers this region. Multiple plants achieve this solar share, in order to have a precise choice, another factor had to be decided, which was the minimum PV curtailment, it reflects lower LCOE as well. Plant “E” key parameter and performance indicators are mentioned in table 6. Further discussion will be presented in the “PV-CCGT optimum plants dynamic performance” section.

6.2.3.2. PV-CCGT firm power 6:00-21:00 “F”

In this section, optimization results of PV-CCGT technology in firm power production from 6:00 to 21:00, with a fixed CCGT capacity of 200 MWe, will be discussed thoroughly. The objectives targeted in this optimization are maximum solar share and minimum LCOE, while variating some key parameters, shown in table 3. The results obtained are similar as expected, to that of baseload operation with some interesting differences. The LCOE range in the 6:00 to 21:00 operation is higher than that of the baseload operation. This could be explained as better utilization is achieved during baseload for the same CapEx invested, in other words, higher electricity yield for same capital investment, which directly reflects lower LCOE. Another difference would be the higher solar share, exceeding 50% achieved in the 6:00 to 21:00 operation. This could be explained by the fact that the 6:00 to 21:00 operation, involves a higher percentage of sunny hours to total hours of operation, than from 0:00 to 24:00 (baseload operation). Accordingly if the same exact plant configuration was operated in both dispatch strategies, the solar share will be definitely higher in the 6:00 to 21:00 operation.

The CapEx relation with solar share and LCOE is the exact same as in the baseload case, as shown in figure 39 (a), where higher solar share requires larger PV installed capacities, as shown in figure 39 (b) increasing the solar share from 0%to 41% requires having a PV capacity ranging from 0 to 0.8 times the CCGT capacity, while increasing the solar share an extra 10%, requires double the capacity needed for the first 40%. Consequently, the end result is higher CapEx and LCOE. Higher solar shares will involve higher curtailment as well, due to the same reason mentioned in the baseload case, and as shown in figure 39(c).

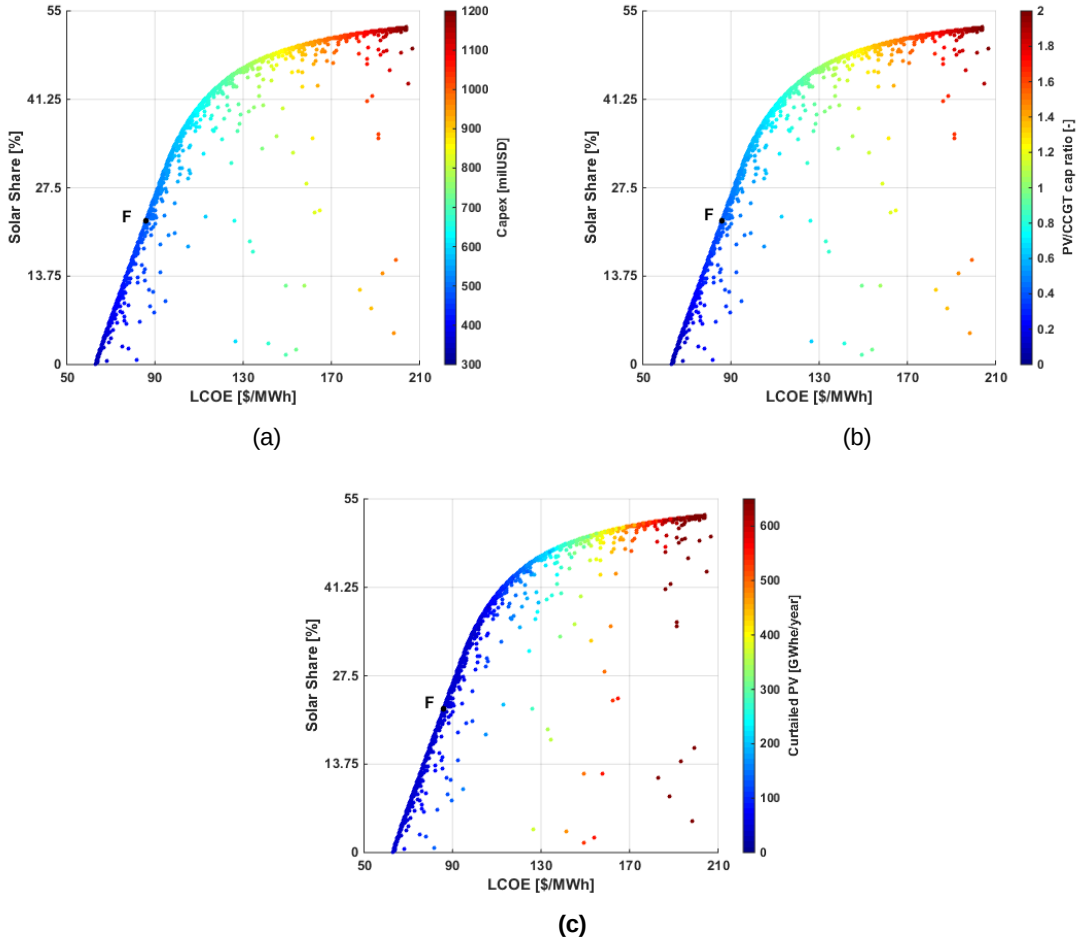

Figure 39. PV-CCGT results in firm power 6:00-21:00 operation: (a) CCGT cap (b) CapEx (c) Curtailed PV

The carbon emissions reduction is directly proportional to solar share, higher solar share results in higher emissions reduction, which is clearly seen in figure 40 (a). The same relation should be applied on operational expenses, the higher the solar share, the less fuel is consumed by the CCGT and accordingly less OpEx. Interestingly enough, this is not the relation obtained. As shown in figure 40(b), the result is the absolute contrary of what expected, the increase in solar share is directly proportional with the OpEx, which means that the hybridization of CCGT with PV, increases the overall OpEx of the plant. It comes off for the extreme of high solar share and high LCOE, where doubling the capacity for PV for an increase of less than 10% of the solar share does not pay-off compared to the corresponding reduction of fuel consumed. While the only explanation for the other extreme of the Pareto front (minimum solar share / minimum LCOE) is that the OpEx associated with the addition of solar capacity is higher than the reduction of OpEx resulting on the CCGT side.

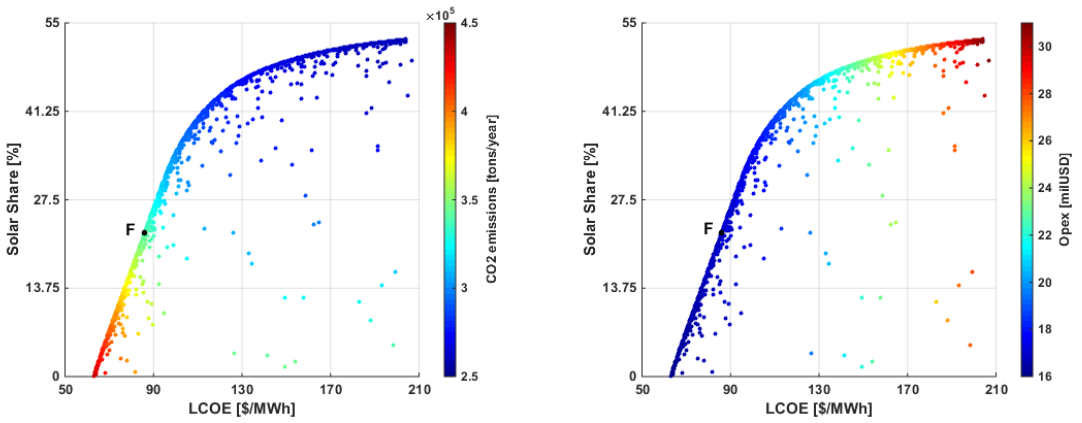

Figure 40. PV-CCGT results in firm power 6:00-21:00 operation: (a) CO2 emissions (b) OpEx

Figure 41 (a) shows the variation of the capacity factor, with increasing the solar share. The plot shows a reduction of the capacity factor with increasing solar share, as mentioned earlier the expected performance was that the capacity factor would be fixed to a value close to that corresponding to the needed operating hours. In this case, 6:00 to 21:00 would account for a CF of 62.5%. The configurations with zero solar share shows a capacity factor of about 55%, which is considered reasonable after accounting for daily starting and shutdown time, in addition to the plant availability. Yet, the CF goes down to nearly 51% with higher solar shares. This is coherent to the result shown in figure 41(b), where the net fuel efficiency drops to 35% from a 48% on a solar share range of 0% to slightly more than 50%.

This could be explained by a model limitation, where the PV production is predefined at each time step, before the dynamic simulation of the power plant, as explained earlier, and according to the PV production the needed Output from the GT is dictated and fed to the GT as the nominal capacity at this time step. Upon which the GT ramps down to be replaced by PV production, and the opposite happens when the PV production start declining. The hybridization of the CCGT and the PV takes place between the PV and the GT, while the ST follows the result of the GT ramping up or down, while the PV production replaces that of the GT and not the ST, and excess production is clipped, at which the max. production of the PV is limited by the capacity of the GT excluding the min, load of operation. That is why there is a drop in the total power O/P of the plant during PV production.

Another reason for the low performance of the model is due to temperature, where high ambient temperature affects two main parts of the CCGT. The first part is the condenser which rejects the heat from the cycle to the ambient, and in dry cooled condenser this process involves cooling down with ambient air. Accordingly higher temperature will reduce the temperature difference and accordingly the rate of heat rejection, which directly impacts the overall efficiency of the cycle. The second part affected is the Gas turbine. Air density decreases with high temperature, affecting the air mass intake of the compressor and the

overall performance of the GT. This performance deterioration will be clearly elaborated in the comparative analysis section.

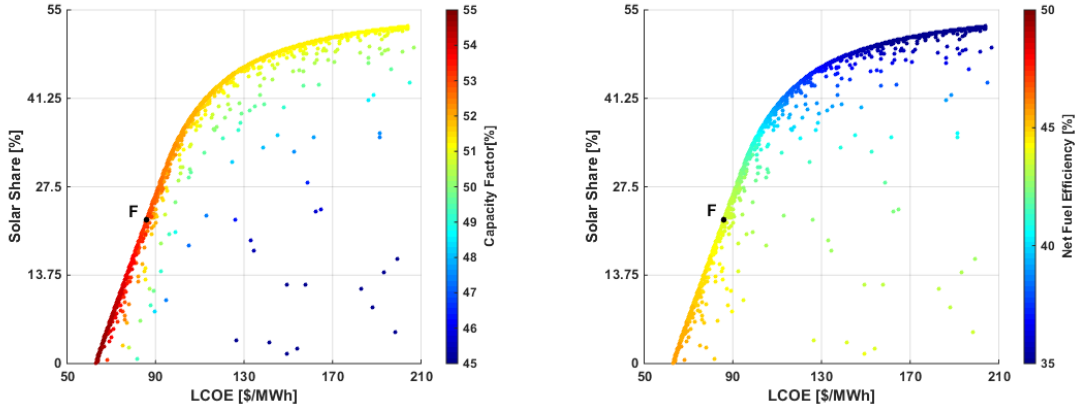

Figure 41. PV-CCGT results in firm power 6:00-21:00 operation: (a) Capacity factor (b) Net Fuel Efficiency

Plant “F” was chosen as an optimum plant for PV-CCGT technology in firm power 6:00 to 21:00 operation. The choice was based on a CF of 53.1%, which is 85% of the maximum theoretical CF (62.5%) of the firm power case. This CF was targeted, as it gives a compromise between solar share, capacity factor and net fuel efficiency, which was concluded after a thorough study of the optimum plants generated by this optimization. Multiple plants achieve this CF, in order to have a precise choice, another factor had to be decided, which was the maximum solar share for this CF. Plant “F” key parameter and performance indicators are mentioned in table 6. Further discussion will be presented in the following section (PV-CCGT optimum plants dynamic performance).

6.2.3.3. PV-CCGT optimum plants dynamic performance:

In this section the PV-CCGT optimum plants selected for each dispatch strategy will be discussed in deeper details considering their key parameters and dynamic performance of a 1 week operation. The same week used for the analysis of CSP and PV-CSP technologies is fixed for PV-CCGT plants analysis, as it provides a significant variation of solar resource, and in order to perform a comparative analysis on same bases. Table 6 shows the key design parameters of the plants under study in both dispatch strategies. As mentioned earlier these plants are not the absolute optimum plants for this technology in this case study, but these are of the optimum plants selected from the Pareto front of the optimizations performed.

Variable	*E*	*F*	*Unit*
Plant type	PV-CCGT	PV-CCGT	[-]
CCGT capacity	396	200	[MWe]
Min. Turbine load	10	10	[%]
PV capacity	399	82	[MWac]
Tracking	Single-Axis	Single-Axis	[-]
Dispatch strategy	Baseload	6:00-21:00	[-]
KPIs and key figures	***E***	***F***	***Unit***
CF	90.3	53.1	[%]
Solar share	28.96	22.41	[%]
PV/CCGT cap. ratio	1.01	0.41	[-]
Electricity production	3132.3	930.25	[GWhe/Year]
CO_2 emissions	1092606	341006	[tons/year]
Net Fuel Efficiency	42.6	43.7	[%]
Curtailed PV	308.64	43.5	[GWhe/Year]
Natural gas price	1	1	[USD/MMBtu]
LCOE	72.8	86.04	[USD/MWhe]
CapEx	1316.6	490.1	[milUSD]
OpEx	57	16.96	[milUSD/Year]
CCGT specific cost	1096	1541	[USD/KWe]
PV specific cost	1801	1801	[USD/KWe]
Plant Specific cost	1486	1628	[USD/KWe]

Table 6. PV-CCGT optimum plants parameters and key figures

Figure 42 shows the dynamic performance of plant E, a PV-CCGT plant in baseload operation. The plant is of 396 MW capacity and hybridized with a 399 MW PV plant, with a minimum loading of 10% of the GT load. The 1 year performance simulation resulted in a CF of 90%, with an electricity production of about 3132 GWhe.

The dynamic performance shows the operation of the plant, with the net electrical output, LP turbine output, HP turbine output, PV power, and net GT output, represented in green, red, blue, yellow and black lines respectively. It is clearly shown that the PV availability dictates the operation of the plant, as according to the PV output the desired load from the GT is defined, with the only constrain in the contribution of the PV is limited to the minimum loading of the GT. Periodic troughs are observed in the net electrical output, these troughs are created during the same duration of PV contribution. This defect has been explained in the reasoning behind low CF. In this section, it will be better elaborated through the plot in figure 42. As shown, the trough on the green line, represents the drop in the output of both the LP and HP of the steam turbine in the CCGT, as the PV production should account for this drop before any curtailment takes place, while still the GT min. load is respected. It could be clearly seen that the troughs in the net electrical output has the exact same shape of the HP and LP troughs summed together.

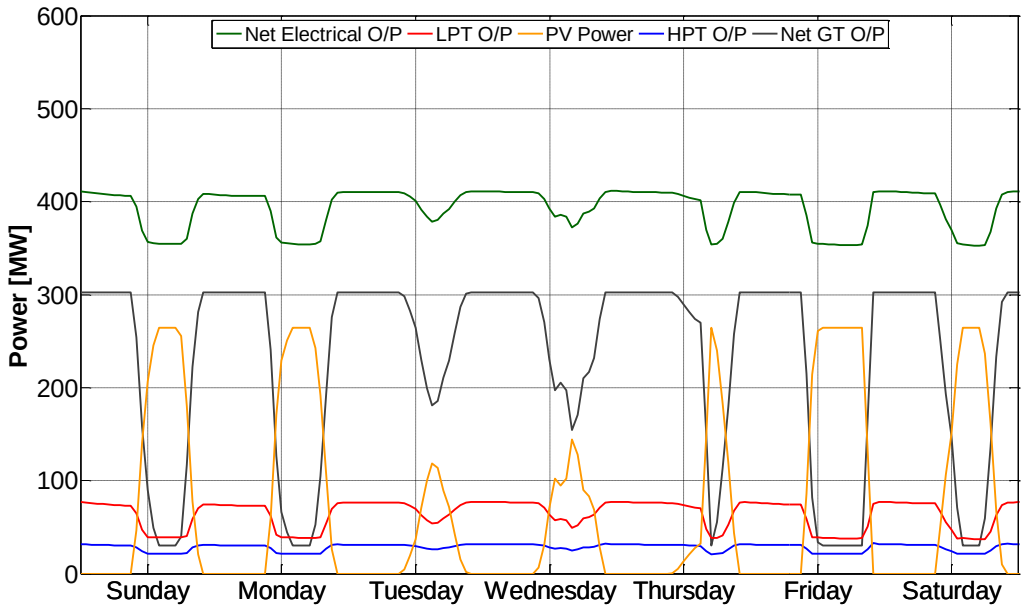

Figure 42. Plant E - PV-CCGT baseload winter week

The second issue mentioned in the results section affecting the overall CF of the plant could be explained if the output plot of figure 43 is compared to that in figure 42, it is the exact same power plant but in a different week, a summer week. The net electrical output is lower than that achieved during a winter week. This is due to the impact of high temperature, as explained in the results section, where the output of the whole CCGT is affected, as the heat rejection from air-cooled condenser is less effective at high temperatures when the temperature difference becomes smaller. On the other hand, the gas turbine air mass intake is affected due to high temperature as mentioned earlier in the results section. Finally, the thermo-economic calculations resulted in a total CapEx of 1317 milUSD, OpEx of 57 milUSD, and an LCOE of 73 USD/MWhe.

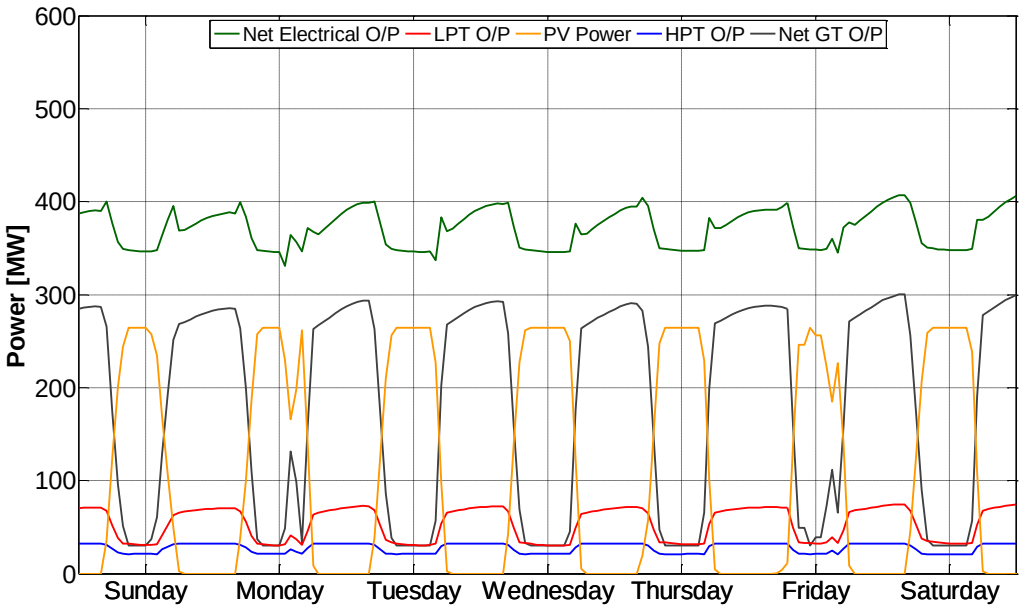

Figure 43. Plant E - PV-CCGT baseload Summer week

Figure 44 shows the performance of plant “F”, a PV-CCGT plant with 200 MW capacity of CCGT, hybridized with 82 MW of PV. The plant is operating from 6:00 to 21:00 providing firm power of 200 MW, with a minimum loading of 10% of the GT load. The 1 year performance simulation resulted in a CF of 53%, with an electricity production of about 930 GWhe.

The dynamic performance shows the operation of the plant during a winter week, same legend as the baseload operation plot in figure 42 and 43. Same comments as in baseload operation are observed clearly. The thermo-economic calculations resulted in a total CapEx of 490.1 milUSD, OpEx of 17 milUSD, and an LCOE of 86 USD/MWhe.

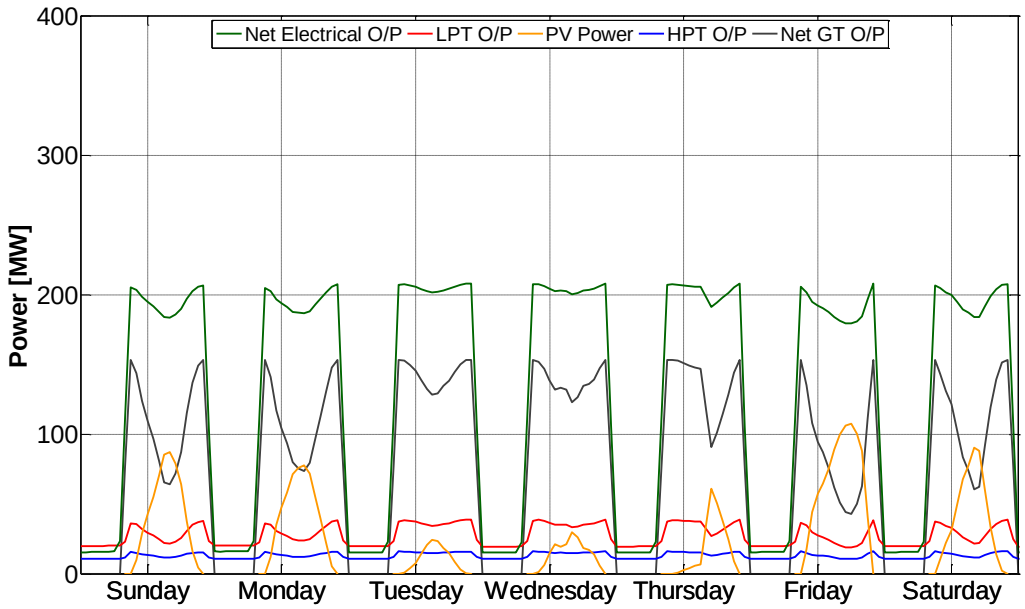

Figure 44. Plant F - PV-CCGT 6:00 to 21:00 operation winter week

7. Comparative analysis

In this section the 3 optimum plants B, D and F, chosen from the 3 technologies CSP, PV-CSP and PV-CCGT, respectively, will be compared against each other. As shown in table 7, the 3 plants are of fixed capacity of 200 MWe, serving a firm power output of 15 hours from 6:00 to 21:00. The 3 plants achieve a CF of 53.1%. Plants B and D provide a 100% renewable, clean generation while plant F is a hybridized plant, incorporating fossil fuel and eventually carbon emissions.

On comparing plants B (CSP) and plant D (PV-CSP) a significant reduction in SM and TES size, where the SM is reduced by about 40%, while the TES is reduced by 54%. This reduction is the result of the hybridization of the 200 MW CSP plant with a 155 MWac PV plant. The PV plant significantly contributed to the desired generation during the day while the CSP plant provided the rest, and charged the storage tanks which serves the load night hours or those with poor irradiance. This hybridization resulted in a much smaller solar field – which is the most CapEx intensive block in the CSP plant - and storage.

Variable	***B***	***D***	***F***	***Unit***
Plant type	CSP	PV-CSP	PV-CCGT	[-]
CSP capacity	200	200	-	[MW]
SM	3.23	1.97	-	
# of Heliostats	32290	17746	-	
Tower height	280	261	-	
TES size	24	11	-	
CCGT capacity	-	-	200	[MWe]
Min. Turbine load	-	-	10	[%]
PV capacity	-	155	82	[MWac]
Tracking	-	Single-Axis	Single-Axis	[-]
Dispatch strategy	6:00-21:00	6:00-21:00	6:00-21:00	[-]
KPIs and key figures	***B***	***D***	***F***	***Unit***
CF	53.1	53.1	53.1	[%]
Solar share	100	100	22.41	[%]
Electricity production	930.36	930.1	930.25	[GWhe/Year]
CO_2 emissions	-	-	341006	[tons/year]
Net Fuel Efficiency	-	-	43.7	[%]
Curtailed PV	-	2.25	43.5	[GWhe/Year]
Natural gas price	-	-	1	[USD/MMBtu]
LCOE	192.78	173.9	86.04	[USD/MWhe]
CapEx	1268.1	763.6	490.1	[milUSD]
OpEx	19.5	13.4	16.96	[milUSD/Year]
CCGT specific cost	-	-	1541	[USD/KWe]

Table 7. Comparative analysis of the 3 technologies in firm power operation

This resulted in lower CapEx, OpEx and consequently LCOE, where the PV-CSP technology provided 11% reduction in LCOE for same capacity factor. Comparing the two B and D to F, plant F provides the minimum LCOE due to the relatively low CapEx and very low NG price of 1 USD/MMBtu. That is on the expense of generating annual emissions of 341 thousand tons per year. Higher curtailment of PV is observed compared to the PV-CSP plant.

8. Sensitivity analysis

In this section two sensitivity analyses have been performed on the PV-CCGT model, specifically plant “F”. The sensitivities are on natural gas price and carbon taxation.

8.1. Natural gas price

A couple of optimizations were performed with a higher natural gas price, while keeping all other design parameters exactly the same. The natural gas price used in the main optimization was the actual cost of fuel in the UAE as mentioned earlier 1 USD/MMBtu[86], which is much lower than the market price. The natural gas price used in the second optimization is the actual market price which is 2.79 USD/MMBtu[88], resulting in the relation shown in figure 45 (a), while that used in the third optimization was 8 USD/MMBtu[88], which was a peak reached early in 2014, resulting in the relation shown in figure 45 (b). The results shown validates the explanation mentioned in the results and discussion section for figure 40, as by using higher fuel prices (without changing PV OpEx figures) the effect is clear that the OpEx relation starts changing and responds with an overall reduction in plant OpEx with higher solar share, as clearly shown in figure 36 (b) with the high natural gas price.

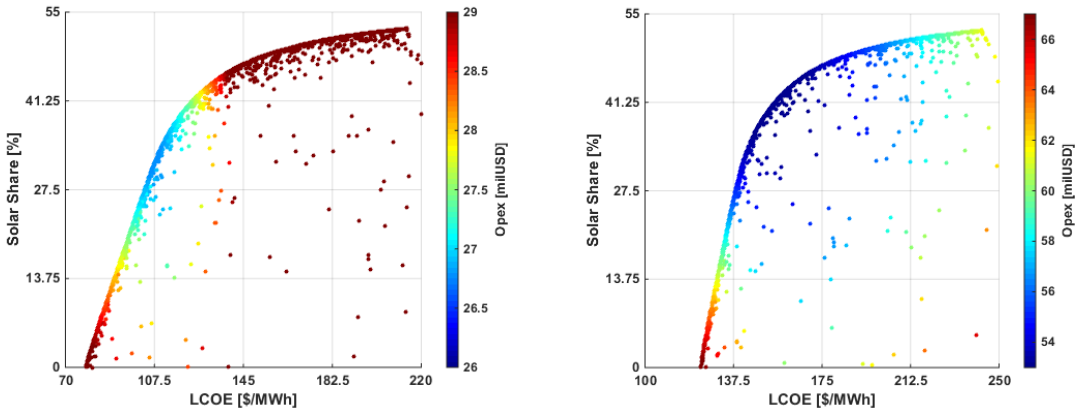

Figure 45. PV-CCGT results in 6:00-21:00 operation - OpEx: (a) NG 2.79 USD/MMBtu (b) NG 8USD/MMBtu

Case	1	2	3	Unit
NG price	1	2.79	8	[USD/MMBtu]
OpEx	3.23	27.2	57	[milUSD]
LCOE	86	98	136	[USD/Mwhe]

Table 7. Natural gas price sensitivity - PV-CCGT 6:00 to 21:00 firm power

This sensitivity analysis shows clearly the impact of considering the actual market price in comparing the competitiveness of renewable energy solutions with fossil fired ones in Countries rich in NG resources, where the cost of NG production is quite low. It is clearly

shown as well that the increase in natural gas market price will lead to competitiveness improvement for CSP related solutions, as shown in table 8, LCOE of the exact same CCGT plant and solar share rises from 86 to 136 USD/MWhe, when comparing with the latest price peak reached since 2014.

8.2. Carbon Tax

The second sensitivity performed on the same exact model and design variables at NG price of 1 USD/MMBtu, while only variating CO2 tax. In order to simulate the impact on LCOE if carbon tax policy is implemented in the UAE, two cases were adopted, the UK and Chile. According to [89], The UK's carbon price floor (CPF) is a tax applied on fossil fuels used to generate electricity. It was implemented in April 2013. In Chile, it is a part of legislation enforced in 2014, where measurements of carbon dioxide emissions from utility scale fossil fired plants will start in 2017, while the tax implementation should start in 2018 on the power sector. The impact of the two adopted policies of the UK and Chile are shown on the plot in figure 46, with the red triangle and green circle, respectively. The plot shows a directly proportional, linear relation between LCOE and carbon tax, as all other parameters are kept constant.

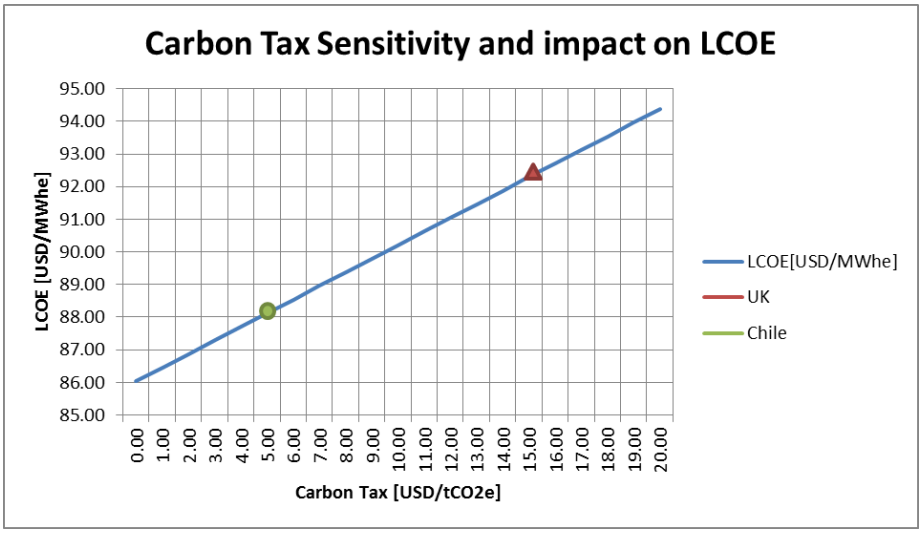

Figure 46. Carbon Tax sensitivity and impact on LCOE

The impact of implementing a carbon tax is obvious from table 9, where the LCOE has risen with about 8%, considering the extreme case (UK).

Country	Tax	Unit	LCOE	Imp.
UAE	0	USD/tCO2e	86	-
Chile	5	USD/tCO2e	88	2018
UK	15.75	USD/tCO2e	92	2014

Table 8. Carbon Tax sensitivity and impact on LCOE

Carbon emissions calculated in this model represents CO2 emissions only and not other emissions as NOx, while the tax is applied per ton CO2 equivalent. Accordingly a precise calculation for the emissions generated from NG consumed will reflect higher LCOE.

9. Conclusion

The objective of this work was to study the competitiveness of CSP and PV-CSP technologies in the MENA region and benchmark it with hybridized PV-CCGT considering current tender conditions and market perspectives. Accordingly, techno-economic models have been developed for this objective; optimization cases were prepared in ordered to identify the optimum configuration for each of the studied technology while maintaining a fixed capacity and choosing the same capacity factor for all three technologies.

From the results and comparative analysis discussed in section 7, it could be concluded that the PV-CSP technology is more competitive than CSP technology where the former provided 11% reduction in LCOE compared to the later. As well as a significant reduction in CapEx that represents a reduction of about 40%. The PV-CSP technology provided a better option generally, and specifically for the UAE due to the high concentration of aerosols which impacts the DNI and has much less impact on GHI and accordingly the PV technology would perform better in this case.

The PV-CCGT provided a highly competitive option with the least LCOE representing 55% less than the CSP and 50% less than the PV-CSP technology. The low LCOE achieved by the PV-CCGT is mainly due to the very low price of NG used in this study which represents the actual cost of NG on the government. This low LCOE comes on the expense of carbon emissions were the optimum plant selected resulted in 341 thousand tons of CO2, while having a solar share in electricity production of 22%. Higher NG prices has been implemented in further sensitivity analysis resulting in a significant rise in the PV-CCGT LCOE reaching 136 USD/MWhe, at NG price of 8 USD/MMBtu.

In baseload optimizations performed without fixing the plant capacity, CSP technology converged to capacities ranging between 50 and 150 MW, where lower capacities were favored for higher CF and LCOE, and the opposite for lower CF and LCOE. The PV-CSP technology optimization converged to the same capacity range as the CSP, while achieving higher CF range, with PV/CSP capacity ratio ranging from 0.5 to 1 and higher than 1 for higher CF and LCOE. Finally the PV-CCGT technology optimization converged to capacities higher than 500 MW, for low LCOE and low SS, and to capacities in the range of 150 to 220 MW for higher SS and LCOE, while the trade-off was around 400 MW. This is due to the significant impact of economy of scale associated with the CCGT block.

Competitiveness of Renewable energy solutions is highly impacted with fossil fuel prices, and accordingly to improve the competitiveness of such technologies and stimulate the private sector in contributing in such technologies, reforming energy subsidies is crucial.

10. Suggested Future Improvements

Finally in this section, some work of improvements will be suggested with regards to the developed model and the study in general, that due to time constraints it was not possible to include them in this study.

Model related improvements:

- Improve hybridization of PV to be linked to CC and account for ST power shortage, which will provide a smooth firm output of the whole plant.
- Increase the complexity of the GT and the Rankine bottoming cycle, such as optimum steam bleeds, feed water heaters, reheat, and multiple GTs integration.
- Hybridization through a PID or Iterative feedback controllers aiming for better system performance in the hybridization part.

- Integration of waste heat recovery systems for desalination or other purposes to improve CSP competitiveness, which is a very common application in the region of concern of this study.

11. References

[1] K. Larchet and K. Larchet, "Solar PV-CSP Hybridisation for Baseload Generation A Techno-economic Analysis for the Chilean Market," 2015.

[2] J. Spelling, "Thermo-economic Evaluation of Solar Thermal and Photovoltaic Hybridization Options for Combined-Cycle Power Plants," vol. 137, no. March, pp. 1–11, 2015.

[3] L. R. C. O, "Techno-economic Analysis of Combined Hybrid Concentrating Solar and Photovoltaic Power Plants : a case study for optimizing solar energy integration into the South African electricity grid," 2014.

[4] U.S Energy Information Administration, *International Energy Outlook 2016*, vol. 484, no. May. 2016.

[5] IEA, "Energy and climate change," *World Energy Outlook Spec. Rep.*, pp. 1–200, 2015.

[6] D. Y. Goswami and S. M. Besarati, "Energy Resources: Solar," *World Energy Counc. 2013 World Energy Resour. Sol.*, pp. 1–28, 2013.

[7] S. A. Kalogirou, *Introduction*. 2014.

[8] R. Guédez, M. Topel, J. Spelling, and B. Laumert, "Enhancing the profitability of solar tower power plants through thermoeconomic analysis based on multi-objective optimization," *Energy Procedia*, vol. 69, no. 0, pp. 1277–1286, 2015.

[9] A. Green, "A TECHNO-ECONOMIC ANALYSIS OF HYBRID CONCENTRATING SOLAR POWER AND SOLAR PHOTOVOLTAIC POWER PLANTS FOR FIRM POWER IN MOROCCO," pp. 1–17.

[10] T. K. Ibrahim and M. N. Mohammed, "Thermodynamic Evaluation of the Performance of a Combined Cycle Power Plant," vol. 1, no. 2, pp. 60–70, 2015.

[11] WEC, "World Energy Resources: 2013 survey," *World Energy Counc.*, p. 11, 2013.

[12] C. Richter, S. Teske, and R. Short, "Concentrating Solar Power - Global Outlook 09," pp. 1–88, 2009.

[13] Estela, Greenpeace, and SolarPACES, "Solar Thermal Electricity - Global Outlook 2016," p. 114, 2016.

[14] IEA, "Technology Roadmap Solar Thermal Electricity," *Int. Energy Agency*, p. 52, 2014.

[15] Irena, "Renewable Power Generation Costs in 2012 : An Overview," no. January, p. 92, 2012.

[16] IEA-ETSAP and IRENA, "Concentrating Solar Power Technology Brief," *IEA-ETSAP IRENA Technol. Br. E10*, vol. 1, no. 2, pp. 331–339, 2013.

[17] IEA-ETSAP and IRENA, "Concentrating Solar Power Technology Brief," *IEA-ETSAP IRENA Technol. Br. E10*, vol. 1, no. 2, pp. 331–339, 2013.

[18] K. Chamberlain, "CSP Solar Tower Report 2014 : Cost , Performance and Thermal Storage CSP Solar Tower Report 2014 : Cost , Performance and Thermal Storage Strategically plan your commercial trajectory and optimize profitability in," 2014.

[19] CSP today, "CSP today Global Tracker." [Online]. Available: http://social.csptoday.com/tracker/projects. [Accessed: 01-Jul-2016].

[20] KIC InnoEnergy, "Future renewable energy costs : solar-thermal electricity," p. 43, 2015.

[21] M. J. Montes, A. Ab??nades, J. M. Mart??nez-Val, and M. Vald??s, "Solar multiple optimization for a solar-only thermal power plant, using oil as heat transfer fluid in the parabolic trough collectors," *Sol. Energy*, vol. 83, no. 12, pp. 2165–2176, 2009.

[22] G. Parkinson, "Solar towers and storage – about to change the energy game?," *Reneweconomy*, Jul-2013.

[23] M. Mendelsohn, T. Lowder, and B. Canavan, "Utility-Scale Concentrating Solar Power and Photovoltaics Projects: A Technology and Market Overview," *Natl. Renew. Energy Lab.*, vol. 303, no. April, pp. 275–3000, 2012.

[24] A. J. Sangster, "Solar Photovoltaics," *Green Energy Technol.*, vol. 194, no. 4, pp. 145–172, 2014.

[25] N. Jenkins, *Photovoltaic Systems*, vol. 9, no. 2. 2003.

[26] Fraunhofer ISE, "Current and Future Cost of Photovoltaics. Long-term Scenarios for Market Development, System Prices and LCOE of Utility-Scale PV Systems," *Agora Energiewende*, no. February, p. 82, 2015.

[27] M. Intelligence and F. Series, "PV and Solar Market Intelligence Report Part of Ispy publishing Industry Survey , Market Intelligence and Forecasts Series," vol. 44, no. 0, pp. 1–20, 2013.

[28] IFC, "International Finance Corporation, Utility-Scale Solar Photovoltaic Power Plants - a project Developer's Guide," 2015.

[29] C. Cycle and P. Plants, "Combined Cycle Power Plants," pp. 567–576.

[30] Robert F Boehm; Hongxing Yang; Jinyue Yan, "Handbook of clean energy systems," 2015th ed., Chichester : Wiley, 2015, pp. 870–880.

[31] Ieaghg, "Operating Flexibility of Power Plants with CCS, 2012/6," no. June, p. 817, 2012.

[32] C. Ruchti, H. Olia, K. Franitza, A. Ehrsam, A. Power, and W. Bauver, "Combined cycle power plants as ideal solution to balance grid fluctuations Fast start-up capabilities," *Kraftwerkstechniches Kolloquium*, pp. 1–13, 2011.

[33] IMIA, "Combined Cycle Power Plants," vol. 2012, no. 12/25, 2013.

[34] J. Zachary, "The Role of Simple and Combined Cycles in Renewable Applications Deployment," *Vol. 3 Control. Diagnostics Instrumentation; Educ. Electr. Power; Microturbines Small Turbomachinery; Sol. Brayt. Rank. Cycle*, pp. 665–671, 2011.

[35] H. Emberger, E. Schmid, and E. Gobrecht, "Fast Cycling Capability for New Plants and

Upgrade Opportunities Siemens Power Generation (PG), Germany," *Siemens*, pp. 1–13, 2005.

[36] ABENGOA, "ABENGOA SOLAR - Atacama-1." [Online]. Available: http://www.abengoasolar.com/web/en/plantas_solares/plantas_propias/chile/. [Accessed: 20-Jun-2009].

[37] SolarReserve, "SolarReserve - Copiapó." [Online]. Available: http://www.solarreserve.com/en/global-projects/csp/copiapo. [Accessed: 01-Sep-2016].

[38] IRENA - MASDAR, "IRENA - Global Atlas for Renewable Energy." [Online]. Available: http://irena.masdar.ac.ae/#. [Accessed: 01-Aug-2016].

[39] "Middle East Solar Outlook for 2016," 2016.

[40] S. Africa and S. Arabia, "Today Markets Report 2014 dus Report title liscient temporercia," 2014.

[41] R. E. Mapping, "The UAE Solar Atlas," no. April, 2013.

[42] I. Renewable and E. Agency, "UNITED ARAB," no. April, 2015.

[43] J. Dargin, "The Dubai Initiative," *Addressing UAE Nat. Gas Cris. Strateg. a Ration. Energy Policy*, 2010.

[44] CleanTechnica, "Shams-1 largest CSP project middle east performing better than expected." [Online]. Available: http://cleantechnica.com/2015/01/26/shams-1-largest-csp-project-middle-east-performing-better-expected/.

[45] Masdar, "Masdar city solar-PV plant." [Online]. Available: http://www.masdar.ae/en/energy/detail/masdar-city-solar-pv-plant.

[46] First Solar, "First Solar DEWA FactSheet." [Online]. Available: http://www.firstsolar.com/-/media/Downloads/First-Solar-DEWA-FactSheet-English.ashx.

[47] Lexology, "Lexology," 2016. [Online]. Available: http://www.lexology.com/library/detail.aspx?g=2e8be647-b4f0-46fa-ad19-264250de26e8.

[48] DEWA, "DEWA CSP solar projects to generate 1,000 MW in Mohammed bin Rashid Al Maktoum Solar Park," 2016. [Online]. Available: https://www.dewa.gov.ae/en/about-dewa/news-and-media/press-and-news/latest-news/2016/06/dewa-csp-solar-projects-to-generate.

[49] A. Power and A. Power, "DEWA 200 MW PV – A Case Study."

[50] DEWA, "DEWA announces selected bidder for 800 MW third phase of the Mohammed bin Rashid Al Maktoum solar park," 2016. [Online]. Available: https://www.dewa.gov.ae/en/about-dewa/news-and-media/press-and-news/latest-news/2016/06/dewa-announces-selected-bidder.

[51] D. Sharjah, A. Sabkhat, M. Sabkhat, Al ' S., A. Bih, H. Al Tawiyeen, and A. Sea, "Irrigation in

the Middle East region in figures – AQUASTAT Survey 2008 2 Abu Dhabi," pp. 1–14, 2008.

[52] Oxford Business Group, "The Report: Abu Dhabi 2014," 2014, p. 15.

[53] Santander, "Santander trade portal," 2016. [Online]. Available: https://en.portal.santandertrade.com/analyse-markets/united-arab-emirates/economic-political-outline.

[54] Coface, "Coface." [Online]. Available: http://www.coface.com/Economic-Studies-and-Country-Risks/United-Arab-Emirates.

[55] M. East and N. Africa, "Cleantech Survey Report."

[56] FAOSTAT, "Annual statistics," 2015.

[57] Dubai Supreme Council of Energy, "Dubai SCE." [Online]. Available: http://www.dubaisce.gov.ae/dubai_projected.aspx. [Accessed: 01-Aug-2016].

[58] PWC, "Sunrise in the Desert Solar becomes commercially viable in MENA," *Emirates Sol. Ind. Assoc.*, no. January, pp. 1–9, 2012.

[59] "2014 Statistical Report - Abu Dhabi.pdf." .

[60] DEWA, "DEWA -Takes Energy Saving Campaign to Government Departments." [Online]. Available: https://www.dewa.gov.ae/en/about-dewa/news-and-media/press-and-news/latest-news/2009/08/dewa-takes-energy-saving-campaign-to-government-departments.

[61] RSB - Dubai, "RSB - Dubai," 2014.

[62] S. Sponsors, "The UAE State of Energy Report."

[63] DEWA, "No Title," *Slab tariff*, 2016. [Online]. Available: https://www.dewa.gov.ae/en/customer/services/consumption-services/tariff. [Accessed: 01-Jan-2016].

[64] First Solar Inc, "Phase I , Mohammed bin Rashid Al Maktoum Solar Park, Project Datasheet," p. 1, 2013.

[65] A. Power, "Shuaa Energy - ACWA Power." [Online]. Available: http://acwapower.com/project/shuaa-1/.

[66] DEWA, "DEWA announces Financial Close for 200MW IPP Phase II of the Mohammed bin Rashid Al Maktoum Solar Park," 2015. [Online]. Available: https://www.dewa.gov.ae/en/about-dewa/news-and-media/press-and-news/latest-news/2015/07/dewa-announces-financial-close-for-200mw-ipp-phase-ii-of-the-mohammed-bin-rashid-al-maktoum-solar-pa.

[67] DEWA, "DEWA announces selected bidder for 800 MW third phase of the Mohammed bin Rashid Al Maktoum solar park." [Online]. Available: https://www.dewa.gov.ae/en/about-dewa/news-and-media/press-and-news/latest-news/2016/06/dewa-announces-selected-bidder.

[68] R. Guédez, D. Ferruzza, and D. Ferruzza, "Thermocline Storage for Concentrated Solar

Power Techno-economic performance evaluation of a multi-layered single tank storage for Solar Tower," 2015.

[69] F. Dominio, "Techno-Economic Analysis of Hybrid PV-CSP Power Plants."

[70] F. P. Incropera, D. P. DeWitt, T. L. Bergman, and A. S. Lavine, *Fundamentals of Heat and Mass Transfer*, vol. 6th. John Wiley & Sons, 2007.

[71] P. Krummenacher and D. Favrat, *Intégration énergétique de procédés industriels par la méthode du pincement étendue aux procédés discontinus.* 1995.

[72] P. Gilman, N. Blair, M. Mehos, C. Christensen, S. Janzou, and C. Cameron, "Solar Advisor Model: User Guide for Version 2.0," no. August, p. 133, 2008.

[73] B. L. Kistler, "A user's manual for DELSOL3: A computer code for calculating the optical performance and optimal system design for solar thermal central receiver plants," *Other Inf. Portions this Doc. are illegible Microfich. Prod. Orig. copy available until Stock is exhausted. Incl. 5 sheets 48x Reduct. Microfich.*, p. Medium: X; Size: Pages: 231, 1986.

[74] J. D. Spelling, *Hybrid Solar Gas-Turbine Power Plants A Thermoeconomic Analysis*. .

[75] A. V. T. Schießl, "Implementation and validation of financial models and stochastic price forecasting on an existing solar tower plant optimization tool Eidesstattliche Erklärung," 2015.

[76] NREL, "NREL - SAM Help." [Online]. Available: https://www.nrel.gov/analysis/sam/help/html-php/index.html?mtf_lcoe.htm. [Accessed: 01-Jun-2016].

[77] E. Harder and J. M. Gibson, "The costs and benefits of large-scale solar photovoltaic power production in Abu Dhabi, United Arab Emirates," *Renew. Energy*, vol. 36, no. 2, pp. 789–796, 2011.

[78] D. Chung, C. Davidson, R. Fu, K. Ardani, and R. Margolis, "U . S . Photovoltaic Prices and Cost Breakdowns : Q1 2015 Benchmarks for Residential , Commercial , and Utility-Scale Systems," *Natl. Renew. Energy Lab.*, no. September, 2015.

[79] Pequot Publishing Inc., "Gas Turbine World 2014-15 Handbook - Volume 31," 2015.

[80] I. Statistics, "Updated Capital Cost Estimates for Utility Scale Electricity Generating Plants," no. April, 2013.

[81] Black & Vetch Holding Company, "Cost and Performance data for Power Generation Technologies," *Natl. Renew. Energiy Lab.*, no. February, pp. 1–106, 2012.

[82] NREL, "Natural Gas Combined-Cycle Plant," pp. 1–4, 2007.

[83] U.S. Department of Energy, "Cost Estimation Methodology for NETL Assessments of Power Plant Performance," p. 26, 2011.

[84] B. R. Druce, "The Role of Nuclear Power in the Middle East Electricity Industry," no. October, 2015.

[85] Decc, "Electricity Generation Costs," *Dep. Energy Clim. Chang.*, no. July, p. 68, 2013.

[86] T. I. M. Boersma and S. Griffiths, “Initial Lessons from the United Arab Emirates,” no. January, 2016.

[87] J. Spelling, B. Laumert, and T. Fransson, “Advanced hybrid solar tower combined-cycle power plants,” *Energy Procedia*, vol. 49, pp. 1207–1217, 2014.

[88] EIA, “EIA - U.S. Energy Information Adminstration.” [Online]. Available: https://www.eia.gov/dnav/ng/hist/rngwhhdm.htm. [Accessed: 20-Jun-2008].

[89] D. M. Driesen, “Putting a Price on Carbon: A Comment,” no. October, pp. 1–26, 2013.